NIST Technical Note 1526

Microwave Dielectric Characterization of Unpatterned Thin Films Using a $Te_{0\gamma\nu}$ Mode Dielectric Resonator Technique: Theory

Richard G. Geyer
Clifford Krowne

NIST
National Institute of Standards and Technology
Technology Administration, U.S. Department of Commerce

NIST Technical Note 1526

Microwave Dielectric Characterization Of Unpatterned Thin Films Using A $Te_{0\gamma\nu}$ Mode Dielectric Resonator Technique: Theory

Richard G. Geyer
Radio-Frequency Technology Division
Electronics and Electrical Engineering Laboratory

Clifford Krowne
Electronic Systems and Technology Division
Naval Research Laboratory

August 2002

U.S. Department of Commerce
Donald L. Evans, Secretary

Technology Administration
Phillip J. Bond, Under Secretary for Technology

National Institute of Standards and Technology
Arden L. Bement, Jr., Director

Certain commercial entities, equipment, or materials may be identified in this document in order to describe an experimental procedure or concept adequately. Such identification is not intended to imply recommendation or endorsement by the National Institute of Standards and Technology, nor is it intended to imply that the entities, materials, or equipment are necessarily the best available for the purpose.

National Institute of Standards and Technology Technical Note 1526
Natl. Inst. Stand. Technol. Tech. Note 1526, 42 pages (August 2002)
CODEN: NTNOEF

U.S. GOVERNMENT PRINTING OFFICE
WASHINGTON: 2002

For sale by the Superintendent of Documents, U.S. Government Printing Office
Internet: bookstore.gpo.gov Phone: (202) 512-1800 Fax: (202) 512-2250
Mail: Stop SSOP, Washington, DC 20402-0001

MICROWAVE DIELECTRIC CHARACTERIZATION OF UNPATTERNED THIN FILMS USING A $TE_{0\gamma\nu}$ MODE DIELECTRIC RESONATOR TECHNIQUE: THEORY

RICHARD G. GEYER† and CLIFFORD KROWNE††

†National Institute of Standards and Technology
Radio-Frequency Technology Division
325 Broadway
Boulder, CO 80305
email:geyer@boulder.nist.gov

††Naval Research Laboratory
Electronic Systems and Technology Division, Code 6850.3
4555 Overlook Ave. SW
Washington, DC 20375

An axially layered cylindrical dielectric resonator, composed of a substrate and thin film, is placed into a parallel plate waveguide and operated as an axi-symmetric $TE_{0\gamma\nu}$ resonant-mode structure for microwave dielectric thin-film characterization. Using this mode structure, dielectric properties in the plane of the film can be measured. The presence of a tunable gap in the parallel plate waveguide allows for partial electric field filling factors in the film to be maximized and for characterization of the dielectric thin film over a tunable frequency range. Self-adjoint operator theory is used to solve the differential equations describing the z-dependent field variations and solutions are radially mode-matched. In addition, uncertainty analyses for thin-film permittivity and dielectric loss tangent are presented. Unpatterned thin-film measurements with this technique may then be compared with those obtained using coplanar waveguide patterned devices.

Key words: dielectric constant; dielectric resonator; loss tangent; microwave measurements; permittivity measurement; relaxation mechanisms; resonance; substrate; unpatterned thin film dielectric measurement

INTRODUCTION

Techniques used in the evaluation of the dielectric properties of thin-film structures are important for many applications. Some of these applications are thin-film dynamic random access memory (DRAM) cells, high-frequency bypass on-chip capacitors for monolithic microwave integrated circuits (MMICs), thin-film phase-shifters and filters.

Above 1 GHz, little is known about thin-film dielectric behavior. At these frequencies, measurements become more difficult due to stray admittance effects around the thin-film deposited structure or as a consequence of the circuit patterning itself. Dielectric properties of thin-film structures often differ appreciably from their bulk counterparts. For example, the real permittivities of thin films are usually smaller and dielectric losses significantly larger than those of corresponding bulk materials. Tunabilities of ferroelectric thin films not only depend on the microstructure of the deposited film, but also on the substrate. These differences may be due to nonuniform strain arising from film-substrate atomic lattice mismatches, film compositional inhomogeneities, film conductivity, film structural imperfections or electronic effects of film-substrate interfaces. In addition, the dielectric properties of unpatterned thin films can differ significantly from their patterned counterparts. Conductor losses from patterning often dominate insertion losses of a circuit structure at microwave frequencies, making it difficult to evaluate fundamental loss relaxation mechanisms occurring in the film and film-substrate structure. In this report a dielectric resonator method is investigated that could be used to evaluate the dielectric properties of unpatterned thin films.

DIELECTRIC RESONATOR TECHNIQUE FOR UNPATTERNED THIN-FILM CHARACTERIZATION

One approach that can be used in dielectric characterization of an unpatterned thin film at microwave frequencies is illustrated in Fig. 1. This model shows a low-loss dielectric resonator with deposited thin film located between the ground planes of a parallel plate waveguide. The experimental setup is similar to the classic Hakki-Coleman [1] or Courtney technique [2] except that a gap exists between the top of the thin film and the upper ground plane to maximally affect resonant electric field structure in the film.

In general, use of a specimen in a dielectric resonator configuration is a commonly used approach for accurate complex permittivity evaluation of low-loss materials [3]. Dielectric resonator techniques, when applicable, usually provide higher accuracies than other resonant cavity methods because partial electric filling factors for an

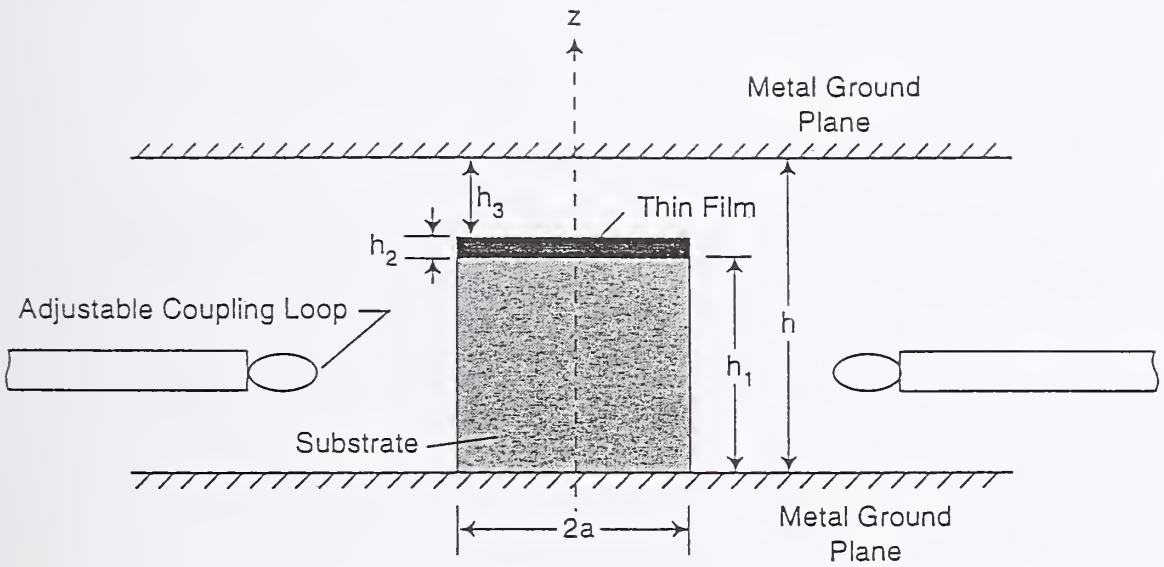

Figure 1: Dielectric resonator system for microwave thin-film measurement.

appropriately chosen mode structure and practically sized specimens are greater, often by a factor of 30 to 100. Uncertainties in various dielectric resonator system techniques typically depend on geometric parameters of the specimen and the relative uncertainty with which resonant frequency is measured for real permittivity evaluation. For dielectric loss evaluation, uncertainties will largely depend on the relative uncertainties with which conductor losses are determined, as well as any coupling or radiation losses. Additionally, loss tangent uncertainty will depend on the measurement accuracy of the unloaded Q-factor at the resonant mode of operation.

The introduction of a gap between the thin-film specimen and the upper ground plane greatly increases the difficulty of analyzing the electromagnetic fields in the composite structure. The electromagnetic fields in each partial region of the composite dielectric resonator structure can be treated as a superposition of transverse magnetic (TM or E-mode) and transverse electric (TE or H-mode) constituents. Boundary conditions on tangential electric and magnetic field components are applied at the cylindrical and axial boundaries and the determinant of a matrix is derived as the eigenvalue equation.

Because introduction of a gap leads to radiative TM and hybrid modes, we consider here the dominant axi-symmetric $\mathrm{TE}_{0\gamma\nu}$ mode ($0 < \gamma < 1$ and $0 < \nu < 1$) which is evanescent in the regions exterior to the axially layered dielectric resonator.

We recall that Maxwell's equations in source-free regions for $e^{j\omega t}$ time dependence are

$$\nabla \times \vec{H} = j\omega\epsilon^* \vec{E}, \tag{1}$$

$$\nabla \times \vec{E} = -\frac{\partial \vec{B}}{\partial t} = -j\omega\mu^* \vec{H}, \tag{2}$$

$$\begin{aligned} \nabla \cdot \vec{B} &= \nabla \cdot (\mu^* \vec{H}) \\ &= \nabla\mu^* \cdot \vec{H} + \mu^* \nabla \cdot \vec{H} \\ &= 0, \end{aligned} \tag{3}$$

$$\begin{aligned} \nabla \cdot \vec{D} &= \nabla \cdot (\epsilon^* \vec{E}) \\ &= \nabla\epsilon^* \cdot \vec{E} + \epsilon^* \nabla \cdot \vec{E} \\ &= 0, \end{aligned} \tag{4}$$

where $\epsilon^* = \epsilon_0 \epsilon_r^*$ is the complex permittivity, $\mu^* = \mu_0 \mu^*$ is the complex permeability, $\epsilon_r^* = \epsilon_r'(1 - j \tan\delta)$ is the relative complex permittivity with real permittivity ϵ_r' and dielectric loss tangent $\tan\delta$, and where $\mu_r^* = \mu_r'(1 - \tan\delta_m)$ is the relative complex permeability with real permeability μ_r' and magnetic loss tangent $\tan\delta_m$;

$\epsilon_0 = 8.854 \times 10^{-12}$ F/m and $\mu_0 = 4\pi \times 10^{-7}$ H/m are the free space permittivity and permeability, and $\omega = 2\pi f$ is the angular frequency.

Equations (1) through (4) are valid for charge-free materials having linear, isotropic permittivity and permeability. If the medium is dielectrically and magnetically homogeneous, eqs (3) and (4) can be written as

$$\nabla \cdot \vec{H} = 0 \tag{5}$$

and

$$\nabla \cdot \vec{E} = 0. \tag{6}$$

The vector Helmholtz equations are readily derived from eqs (1), (2), (5), and (6) and the vector identity $\nabla \times \nabla \times \vec{A} = \nabla(\nabla \cdot \vec{A}) - \nabla^2 \vec{A}$; i.e.,

$$(\nabla^2 + k^2)\vec{E} = 0, \tag{7}$$

and

$$(\nabla^2 + k^2)\vec{H} = 0, \tag{8}$$

where $k^2 = \omega^2 \mu^* \epsilon^*$.

In general, eqs (7) and (8) can be resolved into three scalar Helmholtz equations when solving electromagnetic field problems. However, the level of difficulty can be reduced by noting that only two field components are needed to derive all other components. In cylindrical coordinates these may be the axially-directed E_z (E-mode or TM) and H_z (H-mode or TE) components.

In cylindrical coordinates (r,ϕ,z) the curl operator on a vector $\vec{A}$ is

$$\begin{aligned} \nabla \times \vec{A} &= \frac{1}{r} \begin{vmatrix} \hat{a}_r & r\hat{a}_\phi & \hat{a}_z \\ \frac{\partial}{\partial r} & \frac{\partial}{\partial \phi} & \frac{\partial}{\partial z} \\ A_r & rA_\phi & A_z \end{vmatrix} \\ &= \hat{a}_r \left(\frac{1}{r}\frac{\partial A_z}{\partial \phi} - \frac{\partial A_\phi}{\partial z} \right) + \hat{a}_\phi \left(\frac{\partial A_r}{\partial z} - \frac{\partial A_z}{\partial r} \right) \\ &\quad + \hat{a}_z \frac{1}{r} \left[\frac{\partial}{\partial r}(rA_\phi) - \frac{\partial A_r}{\partial \phi} \right], \end{aligned} \tag{9}$$

so that Faraday's and Ampere's laws may be written

$$\frac{1}{r}\frac{\partial E_z}{\partial \phi} - \frac{\partial E_\phi}{\partial z} = -j\omega\mu^* H_r, \tag{10}$$

$$\frac{\partial E_r}{\partial z} - \frac{\partial E_z}{\partial r} = -j\omega\mu^* H_\phi, \tag{11}$$

$$\frac{1}{r}\left[\frac{\partial(rE_\phi)}{\partial r} - \frac{\partial E_r}{\partial \phi}\right] = -j\omega\mu^* H_z, \tag{12}$$

$$\frac{1}{r}\frac{\partial H_z}{\partial \phi} - \frac{\partial H_\phi}{\partial z} = j\omega\epsilon^* E_r, \tag{13}$$

$$\frac{\partial H_r}{\partial z} - \frac{\partial H_z}{\partial r} = j\omega\epsilon^* E_\phi, \tag{14}$$

and

$$\frac{1}{r}\left[\frac{\partial(rH_\phi)}{\partial r} - \frac{\partial H_r}{\partial \phi}\right] = j\omega\epsilon^* E_z. \tag{15}$$

By substitution, all transverse electric and magnetic field components can be written in terms of the axial E_z and H_z components,

$$\left[\frac{\partial^2}{\partial z^2} + k^2\right] E_\phi = \frac{1}{r}\frac{\partial^2 E_z}{\partial z \partial \phi} + j\omega\mu^*\frac{\partial H_z}{\partial r}, \tag{16}$$

$$\left[\frac{\partial^2}{\partial z^2} + k^2\right] H_r = j\omega\epsilon^*\frac{1}{r}\frac{\partial E_z}{\partial \phi} + \frac{\partial^2 H_z}{\partial z \partial r}, \tag{17}$$

$$\left[\frac{\partial^2}{\partial z^2} + k^2\right] H_\phi = -j\omega\epsilon^*\frac{\partial E_z}{\partial r} + \frac{1}{r}\frac{\partial^2 H_z}{\partial z \partial \phi}, \tag{18}$$

and

$$\left[\frac{\partial^2}{\partial z^2} + k^2\right] E_r = \frac{\partial^2 E_z}{\partial z \partial r} - j\omega\mu^*\frac{1}{r}\frac{\partial H_z}{\partial \phi}, \tag{19}$$

where the longitudinal field components must satisfy

$$\left[\nabla^2 + k^2\right] E_z = 0 \tag{20}$$

and

$$\left[\nabla^2 + k^2\right] H_z = 0. \tag{21}$$

Note that $E_z = 0$ for TE modes and $H_z = 0$ for TM modes. For axi-symmetric TE modes, $E_z = H_\phi = E_r = 0$ and for axi-symmetric TM modes, $H_z = E_\phi = H_r = 0$.

The dielectric resonator system illustrated in Fig. 1 contains a relative real permittivity ϵ_r' that is a piecewise-constant function of z. In general, we can choose to represent the field in each partial region as a superposition of the H-mode and E-mode constituents which individually satisfy the boundary conditions at the conductor plates, and in which the sum of the tangential H-mode and E-mode constituents are continuous across boundaries. In this analysis, we will assume that the substrate and thin film are nonmagnetic, so that there is no discontinuity in the longitudinal magnetic field for TE modes across the axial boundaries $z = h_1$ or $z = h_1 + h_2$. From eqs (4) and (6) we recognize that if $\vec{E}$ is TE to z, $\nabla \cdot \vec{E} = 0$, even for the piecewise-constant permittivity function $\epsilon_r'(z)$ of our dielectric resonator system. Hence the electric field can be given by the curl of a z-directed Hertzian potential $\vec{\Pi}$,

$$\vec{E} = -\frac{1}{\epsilon_0} \nabla \times \vec{\Pi}, \tag{22}$$

where

$$\vec{\Pi} = \hat{z}\vec{\Pi}_z = \hat{z}\psi^h(r,z)\cos(m\phi). \tag{23}$$

The superscript h denotes the H-mode potential that generates a TE field transverse to z, which is the solution of the Helmholtz wave equation expressed in cylindrical coordinates,

$$\frac{1}{r}\frac{\partial}{\partial r}\left[r\frac{\partial \psi^h}{\partial r}\right] - \frac{m^2}{r^2}\psi^h + \frac{\partial^2 \psi^h}{\partial z^2} + k_0^2 \epsilon_r^* \psi^h = 0, \tag{24}$$

where $k_0^2 = \omega^2 \mu_0 \epsilon_0$. Equations (16) through (21) demonstrate that any mode structure of the dielectric resonator system shown in Fig. 1 can be decomposed into its TE and TM parts, and that all field components can be derived from the longitudinal electric and magnetic fields. For the dominant axi-symmetric TE resonant frequency, we can show that all field components in all regions are derivable from the azimuthal electric field, $E_\phi(r,z)$, which satisfies the following equation,

$$\frac{\partial^2 E_\phi}{\partial r^2} + \frac{1}{r}\frac{\partial E_\phi}{\partial r} + \left[k^2(z) - \frac{1}{r}\right] E_\phi + \frac{\partial^2 E_\phi}{\partial z^2} \quad = \quad 0, \tag{25}$$

where $k^2(z)$ is the wavenumber equal to $\omega^2 \mu_0 \epsilon_0$ in the regions exterior to the composite dielectric resonator, $\omega^2 \mu_0 \epsilon_0 \epsilon^*_{r,thinfilm}$ in the film, and $\omega^2 \mu_0 \epsilon_0 \epsilon^*_{r,substrate}$ in the substrate.

Note that eq (25) can be written in operator form,

$$D_r E_\phi + D_z E_\phi = 0, \tag{26}$$

where D_r and D_z are the partial differential operators acting on functions of r and z. Because D_z is self-adjoint, E_ϕ can be expanded in a series of orthogonal eigenfunctions $Z_n^h(z)$ of D_z with real eigenvalues [4].

For convenience, we will use the subscripts 1 and 2 to denote the substrate and thin film, respectively. Subscript 3 denotes the region $h_1 + h_2 \leq z \leq h$, with $r \leq a$ and the subscript 4 denotes the region $r \geq a$.

The necessary continuity boundary conditions for fields transverse electric to z that must be satisfied are

$$E_\phi(r,0) = E_\phi(r,h) = 0, \qquad h = h_1 + h_2, \tag{27}$$

$$E_{\phi,2}(r,h_1) = E_{\phi,1}(r,h_1), \qquad 0 \leq r \leq a, \tag{28}$$

$$E_{\phi,3}(r,h_1+h_2) = E_{\phi,2}(r,h_1+h_2), \qquad 0 \leq r \leq a, \tag{29}$$

$$H_{r,1}(r,h_1) = H_{r,2}(r,h_1), \qquad 0 \leq r \leq a, \tag{30}$$

$$H_{r,2}(r,h_1+h_2) = H_{r,3}(r,h_1+h_2), \qquad 0 \leq r \leq a, \tag{31}$$

$$H_{z,1}(a,z) = H_{z,4}(a,z), \qquad 0 \leq z \leq h_1, \tag{32}$$

$$H_{z,2}(a,z) = H_{z,4}(a,z), \qquad h_1 \leq z \leq h_1 + h_2. \tag{33}$$

Since

$$H_r = -\frac{1}{j\omega\mu}\frac{\partial E_\phi}{\partial z} \tag{34}$$

and

$$H_z = -\frac{1}{j\omega\mu}\frac{1}{r}\left[\frac{\partial(rE_\phi)}{\partial r}\right], \tag{35}$$

we note that E_ϕ and $\partial E_\phi/\partial z$ are continuous at $z = h_1$ and $z = h_1 + h_2$ and that E_ϕ, $\partial E_\phi/\partial r$, and $\partial(rE_\phi)/\partial r$ are continuous at $r = a$. In addition, the choice of the radial dependence of E_ϕ must satisfy the Sommerfeld radiation condition as $r \to \infty$ in the region exterior to the dielectric resonator.

Modal Expansions

We divide the model space into two regions, R_{ext} for $r > a$ and R_{int} for $r < a$. In R_{ext}, $k^2(z)$ remains spatially constant and is equal to k_0^2. Hence,

$$E_{\phi,ext}(r,z) = E_{\phi,4}(r,z) = E_\phi(r,z) = \sum_{n=1}^{\infty} B_n K_1(\xi_n^h r) Z_{n,ext}^h(z), \qquad r \geq a \tag{36}$$

where K_1 is the modified Bessel function of order 1, $Z_{n,ext}^h(z) = \sin(n\pi z/h)$, and $\xi_n^h = [(n\pi/h)^2 - k_0^2]^{1/2}$ or $\xi_n^h = -j[k_0^2 - (n\pi/h)^2]^{1/2}$. The TE axial eigenfunctions

$Z^h_{n,ext}(z)$ satisfy the boundary conditions $Z^h_{n,ext}(0) = Z^h_{n,ext}(h) = 0$ in the region exterior to the composite dielectric resonator using eq (27). For nonradiating modes, all values of ξ^h_n are real.

In the region R_{int}, the relevant modal expansions are more complex, since this region is not homogeneous. In R_{int}, $k^2(z)$ is independent of r, so that the operator eq (26) is valid, D_z is self-adjoint, and E_ϕ can be expanded in a series of orthogonal eigenfunctions $Z^h_n(z)$ of D_z with real eigenvalues η^h_n. Hence the azimuthal electric field in R_{int} may be rigorously represented by the eigenfunction expansion,

$$E_\phi(r,z) = \sum_{n=1}^{\infty} A_n J_1(\zeta^h_n r) Z^h_n(z) \qquad 0 \le r \le a, \tag{37}$$

where J_1 is the Bessel function of the first kind, order 1, $\zeta^h_n = (\eta^h_n)^{1/2}$ or $\zeta^h_n = j(-\eta^h_n)^{1/2}$ is the radial wavenumber associated with the nth axial eigenfunction chosen so that η^h_n are the positive real eigenvalues of $Z^h_n(z)$. The TE eigenfunctions are determined by solving the self-adjoint Sturm-Liouville problem

$$\frac{d^2}{dz^2} Z^h_n(z) + \left(k_0^2 \epsilon_r - \eta^h_n\right) Z^h_n(z) = 0, \tag{38}$$

subject to field boundary conditions at axial boundaries for $0 \le r \le a$. For $0 \le r \le a$,

$$\begin{aligned} \epsilon_r(z) &= \epsilon_{r,1}, \qquad 0 \le z \le h_1, \\ &= \epsilon_{r,2}, \qquad h_1 < z < h_1 + h_2, \\ &= 1, \qquad h_1 + h_2 \le z \le h. \end{aligned} \tag{39}$$

Equation (38) has an infinite number of real, discrete eigenvalues [5]. The eigenfunctions $Z^h_n(z)$ can also be made real-valued by multiplying them by appropriate nonzero constants. When properly normalized, they are orthonormal so that

$$\int_0^h Z^h_n(z) Z^h_m(z) dz = < Z^h_n, Z^h_m > = \delta_{mn}, \tag{40}$$

where δ_{mn} is the Kronecker delta equal to 1 when $m = n$ and 0 when $m \neq n$.

In each dielectric region for which $0 \le r \le a$, the axial eigenfunctions will have different functional forms, so that we introduce the notation

$$\begin{aligned} Z^h_n(z) &= \frac{1}{\sqrt{C^h_n}} Z^h_{n,1}(z), \qquad 0 \le z \le h_1 \\ &= \frac{1}{\sqrt{C^h_n}} Z^h_{n,2}(z), \qquad h_1 \le z \le h_1 + h_2 \end{aligned} \tag{41}$$

$$= \frac{1}{\sqrt{C_n^h}} Z_{n,3}^h(z), \qquad h_1 + h_2 \leq z \leq h,$$

where C_n^h are the normalization coefficients that render the eigenfunctions orthonormal with the inner product specified in eq (40).

For each dielectric layer we have

$$\frac{d^2 Z_{n,1}^h}{dz^2} + (k_0^2 \epsilon'_{r,1} - \eta_n^h) Z_{n,1}^h = 0, \tag{42}$$

$$\frac{d^2 Z_{n,2}^h}{dz^2} + (k_0^2 \epsilon'_{r,2} - \eta_n^h) Z_{n,2}^h = 0, \tag{43}$$

$$\frac{d^2 Z_{n,3}^h}{dz^2} + (k_0^2 - \eta_n^h) Z_{n,3}^h = 0. \tag{44}$$

At the perfectly conducting plates the azimuthal electric field E_ϕ vanishes. Hence, by eqs (27) and (37)

$$Z_{n,1}^h(z) = 0, \qquad z = 0, \tag{45}$$

and

$$Z_{n,3}^h(z) = 0, \qquad z = h. \tag{46}$$

Continuity of the tangential electric field E_ϕ across $z = h_1$ and $z = h_1 + h_2$ requires that

$$Z_{n,1}^h(z) = Z_{n,2}^h(z), \qquad z = h_1, \tag{47}$$

and

$$Z_{n,2}^h(z) = Z_{n,3}^h(z), \qquad z = h_1 + h_2. \tag{48}$$

Continuity of the tangential magnetic field H_r across $z = h_1$ and $z = h_1 + h_2$ requires continuity of $\partial E_\phi / \partial z$, or by eqs (30), (32), and (34),

$$\frac{dZ_{n,1}^h(z)}{dz} = \frac{dZ_{n,2}^h(z)}{dz}, \qquad z = h_1, \tag{49}$$

and

$$\frac{dZ_{n,2}^h(z)}{dz} = \frac{dZ_{n,3}^h(z)}{dz}, \qquad z = h_1 + h_2. \tag{50}$$

General solutions to eqs (42) through (44) may be written in each region as

$$Z_{n,1}^h(z) = a_n \sin(\beta_{n,1}^h z), \tag{51}$$

$$Z_{n,2}^h(z) = b_n \sin(\beta_{n,2}^h z) + c_n \cos(\beta_{n,2}^h z), \tag{52}$$

$$Z^h_{n,3}(z) = d_n \sin[\beta^h_{n,3}(z-h)], \tag{53}$$

where $\beta^h_{n,1} = (k_0^2\epsilon'_{r,1} - \eta^h_n)^{1/2}$ or $\beta^h_{n,1} = j(\eta^h_n - k_0^2\epsilon'_{r,1})^{1/2}$; $\beta^h_{n,2} = (k_0^2\epsilon'_{r,2} - \eta^h_n)^{1/2}$ or $\beta^h_{n,2} = j(\eta^h_n - k_0^2\epsilon'_{r,2})^{1/2}$; and $\beta^h_{n,3} = (k_0^2 - \eta^h_n)^{1/2}$ or $\beta^h_{n,3} = j(\eta^h_n - k_0^2)^{1/2}$. Application of the boundary conditions given by eqs (47),(49),and (50) into the latter equations yields the following unnormalized solutions for the TE axial eigenfunctions in each region for $0 \le r \le a$ (see Appendix A),

$$Z^h_{n,1}(z) = a_n \sin(\beta^h_{n,1} z), \tag{54}$$

$$Z^h_{n,2}(z) = a_n \frac{\beta^h_{n,1}}{\beta^h_{n,2}} \cos(\beta^h_{n,1} h_1) \left[\tan\Phi^h_n \cos[\beta^h_{n,2}(z-h_1)] + \sin[\beta^h_{n,2}(z-h_1)]\right] \tag{55}$$

and

$$\begin{aligned} Z^h_{n,3}(z) &= a_n \frac{\beta^h_{n,1}}{\beta^h_{n,3}} \frac{\cos(\beta^h_{n,1}h_1)\cos(\beta^h_{n,2}h_2)}{\cos(\beta^h_{n,3}h_3)} \left[\tan\Phi^h_n \tan(\beta^h_{n,2}h_2) - 1\right] \\ &\cdot \sin[\beta^h_{n,3}(h-z)], \end{aligned} \tag{56}$$

where we have introduced

$$\tan\Phi^h_n = \frac{\beta^h_{n,2}}{\beta^h_{n,1}} \tan(\beta^h_{n,1}h_1). \tag{57}$$

Axial Propagation Constant Equation

The form of the unnormalized axial eigenfunction in the gap expressed by eq (56) was derived by invoking continuity of the radial magnetic field at $z = h_1 + h_2$. Continuity of the azimuthal electric field at $z = h_1 + h_2$ then permits derivation of the axial propagation constant equation. We may rewrite eq (56) at $z = h_1 + h_2$ as

$$\begin{aligned} Z^h_{n,3}(h_1+h_2) &= a_n \frac{\beta^h_{n,1}}{\beta^h_{n,3}} \frac{\cos(\beta^h_{n,1}h_1)\cos(\beta^h_{n,2}h_2)}{\cos(\beta^h_{n,3}h_3)} \left[\tan\Phi_n \tan(\beta^h_{n,2}h_1) - 1\right] \sin(\beta^h_{n,3}h_3) \\ &= a_n \frac{\beta^h_{n,1}}{\beta^h_{n,2}} \cos(\beta^h_{n,1}h_1)\cos(\beta^h_{n,2}h_2) \left[\tan\Phi_n \tan(\beta^h_{n,2}h_2) - 1\right] \\ &\cdot \frac{\beta^h_{n,2}}{\beta^h_{n,3}} \tan(\beta^h_{n,3}h_3), \end{aligned}$$

or

$$Z^h_{n,3}(h_1+h_2) = a_n \frac{\beta^h_{n,1}}{\beta^h_{n,2}} \cos(\beta^h_{n,1}h_1)\cos(\beta^h_{n,2}h_2)\left[\tan\Phi_n \tan(\beta^h_{n,2}h_2) - 1\right] \cdot \tan\Psi_n, \quad (58)$$

where

$$\tan\Psi^h_n = \frac{\beta^h_{n,2}}{\beta^h_{n,3}} \tan(\beta^h_{n,3}h_3). \quad (59)$$

Similarly,

$$\begin{aligned} Z^h_{n,2}(h_1+h_2) &= a_n \frac{\beta^h_{n,1}}{\beta^h_{n,2}} \cos(\beta^h_{n,1}h_1)\left[\tan\Phi_n \cos(\beta^h_{n,2}h_2) + \sin(\beta^h_{n,2}h_2)\right] \\ &= a_n \frac{\beta^h_{n,1}}{\beta^h_{n,2}} \cos(\beta^h_{n,1}h_1)\cos(\beta^h_{n,2}h_2)\left[\tan\Phi_n + \tan(\beta^h_{n,2}h_2)\right]. \quad (60) \end{aligned}$$

Continuity of the tangential electric field $E_{\phi,2} = E_{\phi,3}$ at the $z = h_1 + h_2$ interface then yields

$$Z^h_{n,2}(z) = Z^h_{n,3}(z)\,|_{z=h_1+h_2},$$

or

$$a_n \frac{\beta^h_{n,1}}{\beta^h_{n,2}} \cos(\beta^h_{n,1}h_1)\cos(\beta^h_{n,2}h_2)\left[\tan\Phi_n + \tan(\beta^h_{n,2}h_2)\right] = a_n \frac{\beta^h_{n,1}}{\beta^h_{n,2}} \cos(\beta^h_{n,1}h_1)\cos(\beta^h_{n,2}h_2)\left[\tan\Phi_n \tan(\beta^h_{n,2}h_2) - 1\right]\tan\Psi_n.$$

Hence

$$\tan\Phi^h_n + \tan\Psi^h_n + \tan(\beta^h_{n,2}h_2)\left[1 - \tan\Phi^h_n \tan\Psi^h_n\right] = 0. \quad (61)$$

With the use of the angle-sum relation [6]

$$\tan(x+y) = \frac{\tan x + \tan y}{1 - \tan x \tan y}, \quad (62)$$

eq (61) becomes

$$\tan(\Phi^h_n + \Psi^h_n) + \tan(\beta^h_{n,2}h_2) = 0. \quad (63)$$

We note that Φ_n^h and Ψ_n^h are always real when $\beta_{n,2}^h$ is real, even if $\beta_{n,1}^h$ and $\beta_{n,3}^h$ are imaginary (Appendix B). Therefore, use of the function-sum relation [6]

$$\tan x + \tan y = \frac{\sin(x+y)}{\cos x \cos y} \tag{64}$$

reduces eq (63) to

$$\Phi_n^h + \Psi_n^h + \beta_{n,2}^h h_2 = n\pi, \tag{65}$$

as long as $\cos(\Phi_n + \Psi_n) \neq 0$ and $\cos(\beta_{n,2}^h h_2) \neq 0$. Equivalently,

$$\tan^{-1}\left[\frac{\beta_{n,2}^h}{\beta_{n,1}^h}\tan(\beta_{n,1}^h h_1)\right] + \tan^{-1}\left[\frac{\beta_{n,2}^h}{\beta_{n,3}^h}\tan(\beta_{n,3}^h h_3)\right] + \beta_{n,2}^h h_2 - n\pi = 0,$$
$$n = 0, \pm 1, \pm 2, \pm 3, \ldots \tag{66}$$

In this analysis, we will assume that the thin film under test has the highest real permittivity; that is $\epsilon'_{r,2} > \epsilon'_{r,1}$ and $\epsilon'_{r,2} > 1$. We can then show that the eigenvalues η_n^h are always less than $k_0^2 \epsilon'_{r,2}$ so that $\beta_{n,2}^h$ is always positive real [7]. The axial wavenumbers $\beta_{n,1}^h$ and $\beta_{n,3}^h$ can be expressed in terms of $\beta_{n,2}^h$:

$$\beta_{n,1}^h = \left[(\beta_{n,2}^h)^2 - k_0^2(\epsilon'_{r,2} - \epsilon'_{r,1})\right]^{1/2}, \tag{67}$$

and

$$\beta_{n,3}^h = \left[(\beta_{n,2}^h)^2 - k_0^2(\epsilon'_{r,2} - 1)\right]^{1/2}. \tag{68}$$

Consequently, when eqs (67) and (68) are substituted into eq (66), we obtain a resultant eigenvalue equation in $\beta_{n,2}^h$ for each value of n. We solve eq (66) numerically for $\beta_{n,2}^h$ and compute $\eta_{n,2}^h = k_0^2 \epsilon'_{r,2} - (\beta_{n,2}^h)^2$.

Normalization Constants

Equations (54) through (56) can be used to evaluate the normalization constants C_n^h that make $Z_n^h(z)$ real- valued and an orthonormal set with inner product defined as in eq (40). From eqs (40) and (41), we have

$$\int_0^{h_1} \frac{\left[Z_{n,1}^h(z)\right]^2}{C_n^h} dz + \int_{h_1}^{h_1+h_2} \frac{\left[Z_{n,2}^h(z)\right]^2}{C_n^h} dz + \int_{h_1+h_2}^{h} \frac{\left[Z_{n,3}^h(z)\right]^2}{C_n^h} dz = 1. \tag{69}$$

We can conveniently set $a_n = 1/(\beta^h_{n,1}\sqrt{C^h_n})$ so that

$$\begin{aligned} C^h_n &= \frac{1}{(\beta^h_{n,1})^2} I_1 + \frac{\cos^2(\beta^h_{n,1}h_1)}{(\beta^h_{n,2})^2} I_2 \\ &+ \frac{\cos^2(\beta^h_{n,1}h_1)\cos^2(\beta^h_{n,2}h_2)}{(\beta^h_{n,3})^2\cos^2(\beta^h_{n,3}h_3)} I_3, \end{aligned} \tag{70}$$

where

$$I_1 = \int_0^{h_1} \sin^2(\beta^h_{n,1}z)dz, \tag{71}$$

$$I_2 = \int_{h_1}^{h_1+h_2} \left(\tan\Phi_n \cos\left[\beta^h_{n,2}(z-h_1)\right] + \sin\left[\beta^h_{n,2}(z-h_1)\right]\right)^2 dz, \tag{72}$$

and

$$I_3 = \int_{h_1+h_2}^{h} \sin^2\left[\beta^h_{n,3}(h-z)\right] dz. \tag{73}$$

The integrals I_1, I_2, and I_3 are in standard form (Appendix C), so that the expression for the normalization constants C^h_n may be written as

$$\begin{aligned} C^h_n &= \frac{1}{2(\beta^h_{n,1})^2}\left[h_1 - \frac{\sin(\beta^h_{n,1}h_1)\cos(\beta^h_{n,1}h_1)}{\beta^h_{n,1}}\right] \\ &+ \frac{\cos^2(\beta^h_{n,1}h_1)}{2(\beta^h_{n,2})^2}[h_2(\tan^2\Phi_n + 1) + \frac{\sin(\beta^h_{n,2}h_2)\cos(\beta^h_{n,2}h_2)}{\beta^h_{n,2}}\left(\tan^2\Phi_n - 1\right) \\ &\qquad +2\frac{\tan\Phi_n \sin^2(\beta^h_{n,2}h_2)}{\beta^h_{n,2}}] \\ &+ \frac{\cos^2(\beta^h_{n,1}h_1)\cos^2(\beta^h_{n,2}h_2)}{2(\beta^h_{n,3})^2\cos^2(\beta^h_{n,3}h_3)}\left[\tan\Phi_n \tan(\beta^h_{n,2}h_2) - 1\right]^2\left[h_3 - \frac{\sin(\beta^h_{n,3}h_3)\cos(\beta^h_{n,3}h_3)}{\beta^h_{n,3}}\right]. \end{aligned} \tag{74}$$

Radial Mode Matching

The continuity of E_ϕ and H_z (or $\partial(rE_\phi)/\partial r$ at the radial boundary $r = a$ with the modal eigenfunction expansions given by eqs (36) and (37) must still be enforced. Using the identities [8]

$$\frac{d(yJ_1(y))}{dy} = yJ_0(y), \tag{75}$$

and

$$\frac{d(yK_1(y))}{dy} = -yK_0(y), \tag{76}$$

we obtain

$$\sum_{n=1}^{\infty} B_n K_1(\xi_n^h a)\sin(n\pi z/h) = \sum_{m=1}^{\infty} A_m J_1(\zeta_m^h a) Z_m^h(z), \tag{77}$$

and

$$-\sum_{n=1}^{\infty} \xi_n^h K_0(\xi_n^h a)\sin(n\pi z/h) = \sum_{m=1}^{\infty} \zeta_m^h A_m J_0(\zeta_m^h a) Z_m^h(z), \tag{78}$$

where $Z_n^h(z)$ is given by eq (41) and eqs (54) through (56). If we now take the inner product of each side of eqs (77) and (78) with $Z_m^h(z)$, we obtain

$$\sum_{n=1}^{\infty} B_n K_1(\xi_n^h a) < Z_m^h, \sin(n\pi z/h) >= A_m J_1(\zeta_m^h a), \tag{79}$$

and

$$-\sum_{n=1}^{\infty} \xi_n^h B_n K_0(\xi_n^h a) < Z_m^h, \sin(n\pi z/h) >= \zeta_m^h A_m J_0(\zeta_m^h a), \tag{80}$$

valid for all m. The constant A_m can be eliminated from the above two equations to give

$$\sum_{n=1}^{\infty} B_n[\zeta_m^h J_0(\zeta_m^h a)K_1(\xi_n^h a) + \xi_n^h K_0(\xi_n^h a)J_1(\zeta_m^h a)] < Z_m^h, \sin(n\pi z/h) > \;\; = \;\; 0, \tag{81}$$

also valid for all m. The inner product $< Z_m^h, \sin(n\pi z/h) >$ is given by

$$< Z_m^h, \sin(n\pi z/h) > = \frac{1}{\sqrt{C_m^h}}[\int_0^{h_1} Z_{m,1}^h \sin(n\pi z/h)dz + \int_{h_1}^{h_1+h_2} Z_{m,2}^h \sin(n\pi z/h)dz + \int_{h_1+h_2}^{h} Z_{m,3}^h \sin(n\pi z/h)dz]$$

$$= \frac{1}{C_m^h \beta_{m,1}^h}\tilde{I}_1 + \frac{1}{C_m}\frac{\cos(\beta_{m,1}^h h_1)}{\beta_{m,2}^h}\tilde{I}_2 \quad (82)$$

$$+ \frac{\cos(\beta_{m,1}^h h_1)\cos(\beta_{m,2}^h h_2)}{C_m \beta_{m,3}^h \cos(\beta_{m,3}^h h_3)}\left[\tan\Phi_m \tan(\beta_{m,2}^h h_2) - 1\right]\tilde{I}_3,$$

where

$$\tilde{I}_1 = \int_0^{h_1} \sin(\beta_{m,1}^h z)\sin(n\pi z/h)dz, \quad (83)$$

$$\tilde{I}_2 = \int_{h_1}^{h_1+h_2} \left(\tan\Phi_m \cos[\beta_{m,2}^h(z-h_1)] + \sin[\beta_{m,1}^h(z-h_1)]\right)\sin(\frac{n\pi z}{h})dz, \quad (84)$$

and

$$\tilde{I}_3 = \int_{h_1+h_2}^{h} \sin\left[\beta_{m,3}^h(h-z)\right]\sin(n\pi z/h)dz. \quad (85)$$

The integrals $\tilde{I}_1$, $\tilde{I}_2$, and $\tilde{I}_3$ are evaluated in closed form in Appendix D so that,

$$< Z_m^h, \sin(n\pi z/h) >$$

$$= \frac{h}{C_m^h \beta_{m,1}^h}\frac{\beta_{m,1}^h h\cos(\beta_{m,1}^h h_1)\sin(\frac{n\pi h_1}{h}) - n\pi\sin(\beta_{m,1}^h h_1)\cos(\frac{n\pi h_1}{h})}{(n\pi)^2 - (\beta_{m,1}^h h)^2}$$

$$+\frac{h\cos(\beta_{m,1}^h h_1)}{C_m^h \beta_{m,2}^h}(\tan\Phi_m[\frac{n\pi\left(\cos(\frac{n\pi h_1}{h}) - \cos[\frac{n\pi(h_1+h_2)}{h}]\cos[\beta_{m,2}^h h_2]\right)}{(n\pi)^2 - (\beta_{m,2}^h)^2}$$

$$-\frac{\beta_{m,2}^h h\sin[\frac{n\pi(h_1+h_2)}{h}]\sin(\beta_{m,2}^h h_2)}{(n\pi)^2 - (\beta_{m,2}^h h)^2}]$$

$$+\frac{\beta_{m,2}^h h\left(\cos(\beta_{m,2}^h h_2)\sin[\frac{n\pi(h_1+h_2)}{h}] - \sin(\frac{n\pi h_1}{h})\right) - n\pi\sin(\beta_{m,2}^h h_2)\cos[\frac{n\pi(h_1+h_2)}{h}]}{(n\pi)^2 - (\beta_{m,2}^h h)^2})$$

$$+\frac{h}{C_m^h \beta_{m,3}^h}\frac{\cos(\beta_{m,1}^h h_1)\cos(\beta_{m,2}^h h_2)\left[\tan\Phi_m \tan(\beta_{m,2}^h h_2) - 1\right]}{(n\pi)^2 - (\beta_{m,3}^h h)^2}$$

$$\cdot\left[n\pi\tan(\beta_{m,3}^h h_3)\cos[\frac{n\pi(h_1+h_2)}{h}] + \beta_{m,3}^h h\sin[\frac{n\pi(h_1+h_2)}{h}]\right]. \quad (86)$$

Real Permittivity Evaluation or Resonant Frequency Prediction

Equation (81) represents a infinite system of homogeneous equations. In order for nontrivial solutions to exist, the determinant of the coefficients of matrix [B] must vanish. The real relative permittivity of the thin film may now be evaluated, given the dominant $TE_{0\gamma\nu}$ resonant frequency, dielectric substrate and thin film dimensions, distance between the ground planes of the parallel plate waveguide, real relative permittivity of the substrate, and values of the axial propagation constants determined by the eigenvalue eq (66). Conversely, given the permittivity of the thin film, the resonant frequency may be calculated for a specified gap between the film and upper ground plane of the parallel plate waveguide.

Dielectric Loss Tangent Evaluation

The dielectric loss tangent of the thin film is evaluated from the unloaded Q-factor,

$$\frac{1}{Q_0} = \frac{1}{Q_{tf}} + \frac{1}{Q_p}, \tag{87}$$

where the subscript tf denotes thin film, Q_0 is the unloaded Q-factor, $Q_{tf} = (p_{e,tf} \tan \delta_{tf})^{-1}$ is the thin film quality factor, and $p_{e,tf}$ is the electric energy filling factor of the thin film. The parasitic Q-factor losses, Q_p^{-1}, are given by

$$\frac{1}{Q_p} = p_{e,substrate} \tan \delta_{substrate} + \frac{1}{Q_c} + \frac{1}{Q_r}, \tag{88}$$

where Q_c^{-1} are parallel plate conductor losses, $p_{e,substrate}$, $\tan \delta_{substrate}$ are the electric energy filling factor and loss tangent of the substrate, respectively, and Q_r^{-1} denotes radiative losses. For trapped modes, $Q_r^{-1} = 0$. The partial electric energy filling factor in region i is defined as the ratio of the electric field energy W_i in region i normalized by the *total* electric field energy W in the resonant system; that is,

$$p_{e,i} = \frac{W_i}{W}, \tag{89}$$

where $i = 1, 2, 3, 4$. Note that the total energies in the partial regions and resonant system given in eq (89) are twice the average stored electric field energy, so that the total stored electric energy is obtained by summing separately the electric field energies in each homogenous region,

$$W = \sum_{i=1}^{4} \frac{\epsilon_0 \epsilon'_{r,i}}{2} \int_{V_i} \mid \vec{E}_i \cdot \vec{E}_i^{\,*} \mid dv_i, \tag{90}$$

where $\mid \vec{E}_i \mid$ is the amplitude of the complex electric field in region i. With the resonant system operated in the $TE_{0\gamma\nu}$ dominant mode, only azimuthal electric fields exist. Once the radial wavenumbers ζ_n^h are determined from the eigenvalue eq (66) and the determinant of the matrix $[\mathbf{B}]$ in eq (81), the system of eqs (77) and (78) can be truncated to solve for A_m, B_n $(m = n)$ and the azimuthal electric fields in each region given by eqs (36) and (37).

Another approach for evaluating the partial electric filling factors is to employ the material perturbation theorem [9],

$$p_{e,i} = 2\frac{\epsilon'_{r,i}}{f} \mid \frac{\partial f}{\partial \epsilon'_{r,i}} \mid, \tag{91}$$

where i denotes region 1 (substrate) or region 2 (thin film).

The Q-factor of the resonant system is the ratio of the stored energy to the dissipated power:

$$Q_0 = \frac{2\pi f_0 W}{P_{tot,int}}, \tag{92}$$

where f_0 is the resonant frequency and $P_{tot,int}$ is the total power dissipated in the resonant system, exclusive of any external loading losses in the measurement system. The total dissipated power losses are

$$P_{tot,int} = P_{tf} + P_{substrate} + P_c, \tag{93}$$

where $P_{tf}, P_{substrate}$ are thin film and substrate power losses, and P_c is conductor loss. Equation (87) may then be rewritten as

$$\begin{aligned} \frac{1}{Q_0} &= \frac{P_{tf}}{2\pi f_0 W} + \frac{P_{substrate}}{2\pi f_0 W} + \frac{P_c}{2\pi f_0 W} \\ &= \frac{1}{Q_{tf}} + \frac{1}{Q_{substrate}} + \frac{1}{Q_c}. \end{aligned} \tag{94}$$

We note that the lowest Q of the three terms in eq (94) dominates and is approximately equal to Q_0, particularly if the other two Qs are more than 10 times the smallest Q. The total power P_d dissipated in the dielectric resonant system is obtained by a summation of several integrations performed over each region, similar to eq (90),

$$\begin{aligned} P_d &= \sum_{i=1}^{4} \frac{\sigma_i + \omega\epsilon_0\epsilon''_{r,i}}{2} \int_{V_i} \mid \mathbf{E_i} \cdot \mathbf{E_i^*} \mid dv_i \\ &= \sum_{i=1}^{4} \frac{\sigma_i + \omega\epsilon_0\epsilon''_{r,i}}{2} \int_{V_i} E_{\phi,i}^2 dv_i. \end{aligned} \tag{95}$$

For lossless regions exterior to the composite dielectric resonator, the above summation reduces to two integrations in the substrate and thin film.

The power dissipated in the parallel conductor plates may be determined in the following way. In our resonant system the metals used as ground planes are the same and have the same uniform, isotropic conductivity. At microwave frequencies, the power loss may generally be approximated using the real part of the equivalent surface impedance. For normal metals the surface impedance is

$$Z_s = \frac{1}{\sigma\delta}(1+j), \tag{96}$$

where $\delta = \sqrt{2/(\omega\mu\sigma)}$ is the plane-wave skin depth and σ is the conductivity. The surface resistance is

$$R_s = Re(Z_s) = \frac{1}{\delta\sigma}, \tag{97}$$

The microwave surface resistance of either annealed copper and silver plate that may be used as the metal ground planes of the parallel-plate waveguide are shown in Figs. 2 and 3 as a function of frequency at 297 K. These surface resistance measurements are evaluated with the use of an ultra low-loss c-axis oriented single crystal sapphire dielectric resonator with dimensions for TE_{011} mode resonance (no tunable gap) at 10 GHz [10]. The thickness of copper and silver was large relative to the plane-wave skin depth. For other measurement frequencies the surface resistance is scaled proportionally to the square root of frequency. Hence the power loss in the parallel plate waveguide, which limits the Q-factor, is given by

$$\begin{aligned} P_c &= \frac{1}{2}\int_S R_s \mid \vec{J}_s \cdot \vec{J}_s^{*} \mid dS \\ &= \frac{1}{2}\int_S R_s \mid H_{tan} \mid^2 dS, \end{aligned} \tag{98}$$

where H_{tan} represents the tangential magnetic field at the ground planes that generates the surface current $\vec{J}_s$. If the radius of the ground planes is r_g, the radial magnetic field in each region may be computed from eq (34) and eqs (36) and (37) and integrated in each partial region to give the expression for conductor power loss,

$$\begin{aligned} P_c &= R_s\left[\int_0^{2\pi}\int_0^{a} \mid H_{r,1} \mid^2 r dr d\phi + \int_0^{2\pi}\int_0^{a} \mid H_{r,3} \mid^2 r dr d\phi + 2\int_0^{2\pi}\int_a^{r_g} \mid H_{r,4} \mid^2 r dr d\phi\right] \\ &= 2\pi\left[\int_0^{a}\left(\mid H_{r,1} \mid^2 + \mid H_{r,3} \mid^2\right) r dr + 2\int_a^{r_g} \mid H_{r,4} \mid^2 r dr\right]. \end{aligned} \tag{99}$$

These integrations can be tedious for the numerically derived radial magnetic field components in each region. Another technique that can be used is the incremental inductance rule of Wheeler [11] or incremental frequency rule of Kajfez [12] for

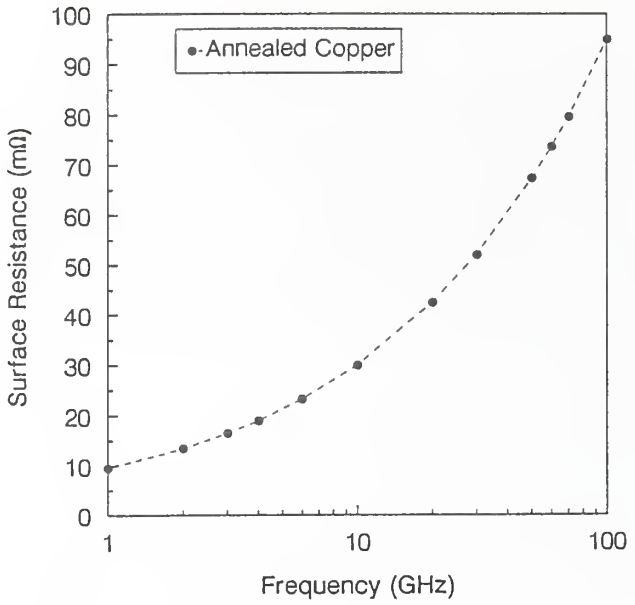

Figure 2: Microwave surface resistance of annealed copper plate as a function of frequency. T = 297 K.

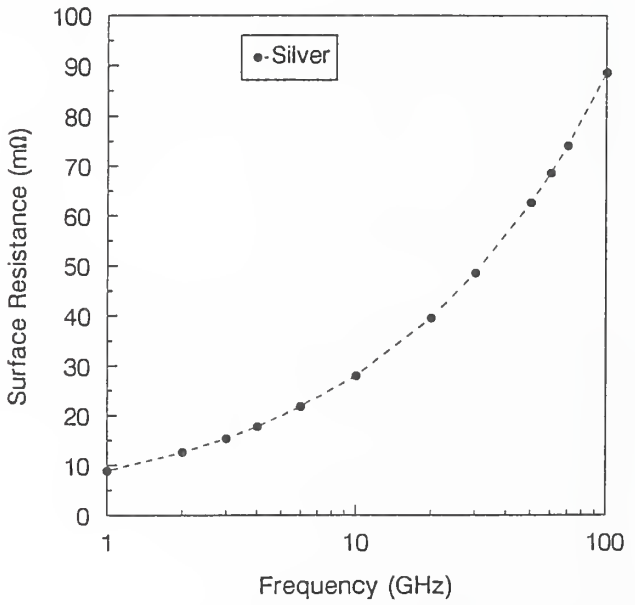

Figure 3: Microwave surface resistance of silver as function of frequency. T = 297 K.

rotationally symmetric modes. To apply this rule, the resonant frequency of the resonant system with perfectly conducting ground planes is computed. Then the ground planes are moved inward by a full skin depth δ. The resulting change in resonant frequency $\Delta f_0(\delta)$ due to this perturbation of the resonant system is computed. The conductor quality factor is then determined from

$$Q_c = \frac{f_0}{\Delta f_0(\delta)}. \tag{100}$$

For completeness, we make one last comment. In practice, a resonant system is always excited by rf coupling feeds that must deliver power to an external load through a coupling port. The power loss due to the presence of an external load in any resonant dielectric measurement system is defined by

$$Q_e = \frac{2\pi f_0 W}{P_e}. \tag{101}$$

The stored energy in the numerator is still the energy stored in the resonant system, but the power loss in the denominator is the external drain on the internal energy. Thus, a loaded quality factor Q_L is always measured, which is the total Q for the system including power losses both internal and external to the resonant system. The loaded Q is given by

$$\frac{1}{Q_L} = \frac{1}{Q_e} + \frac{1}{Q_0}, \tag{102}$$

where Q_0 is given by eq (92). The relationship between Q_0 and Q_L is given by

$$Q_L = \frac{Q_0}{1-\kappa}, \tag{103}$$

where the coupling coefficient $\kappa = P_e/P_{tot,int}$. For a two-port resonant system, $\kappa = \kappa_1 + \kappa_2$. For a single mode two-port resonator with unequal coupling at its input and output, we have

$$Q_0 = Q_L(1 + \kappa_1 + \kappa_2), \tag{104}$$

$$\kappa_1 = \frac{1 - S_{11}}{S_{11} + S_{22}}, \tag{105}$$

$$\kappa_2 = \frac{1 - S_{22}}{S_{11} + S_{22}}, \tag{106}$$

$$S_{21} = S_{12} = \frac{2\sqrt{\kappa_1 \kappa_2}}{1 + \kappa_1 + \kappa_2}, \tag{107}$$

where κ_1 and κ_2 are the coupling coefficients at ports 1 and 2. S_{11}, S_{22}, and S_{21} are the reflection and transmission magnitudes of the scattering S-parameters measured at the resonant frequency f_0. If the coupling at the two-port resonant system is made equal, we simply have

$$Q_0 = \frac{Q_L}{1 - \mid S_{21} \mid}, \tag{108}$$

so that the unloaded Q-factor may be determined from Q_L by measurement of the coupling port insertion losses. This is the first step in any Q-factor measurement for determining the loss tangent of a specimen in a dielectric resonator system.

UNCERTAINTY ANALYSIS

Permittivity

Systematic uncertainties in the determination of $\epsilon'_{r,tf}$ are weakly affected by imperfections of the composite dielectric resonator sample faces, since for TE_0 modes, the electric field has only an azimuthal component that is tangential and contiguous with the resonator surfaces. The relative uncertainty in determining the permittivity of the film with $TE_{0\gamma\nu}$ dominant mode structure may be written in terms of the uncertainties in dielectric resonator radius, substrate height, thin film thickness, gap between film and upper ground plane, real permittivity of substrate and frequency as,

$$\begin{aligned}
\frac{\Delta\epsilon'_{r,tf}}{\epsilon'_{r,tf}} &= [(S_a^{\epsilon'_{r,tf}} \frac{\Delta a}{a})^2 + (S_{h_1}^{\epsilon'_{r,tf}} \frac{\Delta h_1}{h_1})^2 \\
&+ (S_{h_2}^{\epsilon'_{r,tf}} \frac{\Delta h_2}{h_2})^2 + (S_{h_3}^{\epsilon'_{r,tf}} \frac{\Delta h_3}{h_3})^2 \\
&+ (S_{\epsilon'_{r,substrate}}^{\epsilon'_{r,tf}} \frac{\Delta\epsilon'_{r,substrate}}{\epsilon'_{r,substrate}})^2 + (S_f^{\epsilon'_{r,tf}} \frac{\Delta f}{f})^2]^{1/2},
\end{aligned} \tag{109}$$

where

$$S_p^{\epsilon'_{r,tf}} = \frac{p}{\epsilon'_{r,tf}} \frac{\partial\epsilon'_{r,tf}}{\partial p} \tag{110}$$

is the sensitivity of the thin film permittivity relative to the parameter p. The various sensitivity parameters must be numerically evaluated from eq (91).

Dielectric Loss Tangent

The maximum probable uncertainty in dielectric loss tangent of the thin film specimen under test is,

$$\begin{aligned}\Delta \tan\delta_{tf} &= |\,\Delta p_{e,tf}\frac{\partial \tan\delta_{tf}}{\partial p_{e,tf}}\,| + |\,\Delta Q_0\frac{\partial \tan\delta_{tf}}{\partial Q_0}\,| \\ &\quad + |\,\Delta Q_c\frac{\partial \tan\delta_{tf}}{\partial Q_c}\,| + |\,\Delta p_{e,substrate}\frac{\partial \tan\delta_{tf}}{\partial p_{e,substrate}}\,| \\ &\quad + |\,\Delta \tan\delta_{substrate}\frac{\partial \tan\delta_{tf}}{\partial \tan\delta_{substrate}}\,|\,. \end{aligned} \tag{111}$$

The *maximum probable relative uncertainty* in microwave dielectric loss tangent of the thin film may then be written in terms of the relative uncertainties in $p_{e,tf}$, $p_{e,substrate}$, Q_0, Q_c, and $\tan\delta_{substrate}$ and is given by

$$\begin{aligned}\frac{\Delta(\tan\delta_{tf})}{\tan\delta_{tf}} &= |\,\frac{p_{e,tf}}{\tan\delta_{tf}}\frac{\partial \tan\delta_{tf}}{\partial p_{e,tf}}\frac{\Delta p_{e,tf}}{p_{e,tf}}\,| + |\,\frac{Q_0}{\tan\delta_{tf}}\frac{\partial \tan\delta_{tf}}{\partial Q_0}\frac{\Delta Q_0}{Q_0}\,| \\ &\quad + |\,\frac{Q_c}{\tan\delta_{tf}}\frac{\partial \tan\delta_{tf}}{\partial Q_c}\frac{\Delta Q_c}{Q_c}\,| + |\,\frac{p_{e,substrate}}{\tan\delta_{tf}}\frac{\tan\delta_{tf}}{\partial p_{e,substrate}}\frac{\Delta p_{e,substrate}}{p_{e,substrate}}\,| \\ &\quad + |\,\frac{\tan\delta_{substrate}}{\tan\delta_{tf}}\frac{\partial \tan\delta_{tf}}{\partial \tan\delta_{substrate}}\frac{\Delta \tan\delta_{substrate}}{\tan\delta_{substrate}}\,|\,. \end{aligned} \tag{112}$$

The factors multiplying the various parameter relative uncertainties are the sensitivities of the dielectric loss tangent to each of these contributory uncertainties. Hence the rms relative uncertainty in dielectric loss tangent of the thin film specimen is

$$\begin{aligned}\frac{\Delta(\tan\delta_{tf})}{\tan\delta_{tf}} &= [(S_{pe,tf}^{\tan\delta_{tf}}\frac{\Delta(p_{e,tf})}{p_{e,tf}})^2 + (S_{Q_0}^{\tan\delta_{tf}}\frac{\Delta(Q_0)}{Q_0})^2 \\ &\quad + (S_{Q_c}^{\tan\delta_{tf}}\frac{\Delta(Q_c)}{Q_c})^2 + (S_{p_{e,substrate}}^{\tan\delta_{tf}}\frac{\Delta(p_{e,substrate})}{p_{e,substrate}})^2 \\ &\quad + (S_{\tan\delta_{substrate}}^{\tan\delta_{tf}}\frac{\Delta(\tan\delta_{substrate})}{\tan\delta_{substrate}})^2]^{1/2}, \end{aligned} \tag{113}$$

where

$$S_{p_{e,tf}}^{\tan\delta_{tf}} = 1, \tag{114}$$

$$S_{Q_0}^{\tan\delta_{tf}} = 1 + \frac{p_{e,substrate}\tan\delta_{substrate}}{p_{e,tf}\tan\delta_{tf}} + \frac{1}{Q_c p_{e,tf}\tan\delta_{tf}}, \tag{115}$$

$$S_{Q_c}^{\tan\delta_{tf}} = \frac{1}{Q_c p_{e,tf}\tan\delta_{tf}}, \tag{116}$$

$$S^{\tan\delta_{tf}}_{p_{e,substrate}} = S^{\tan\delta_{tf}}_{\tan\delta_{substrate}} = \frac{p_{e,substrate}\tan\delta_{substrate}}{p_{e,tf}\tan\delta_{tf}}. \quad (117)$$

Equation (113) is valid for any resonant system involving a thin film on a substrate, whether dielectric resonator or cavity. Typically, the largest contributions to dielectric loss tangent uncertainty are those due to uncertainties in conductor losses, substrate losses or unloaded Q-factor.

SOLUTION ALGORITHM

We may summarize the solution algorithm as follows:

- Solve axial propagation constant equation for $\beta^h_{n,2}$ for each integer value of n. $\beta^h_{n,1}$ and $\beta^h_{n,3}$ may be written in terms of $\beta^h_{n,2}$ for each integer n. Whether $\beta^h_{n,1}$, $\beta^h_{n,2}$, and $\beta^h_{n,3}$ are real or pure imaginary, reflecting propagating or evanescent modes, depends on substrate, thin film, and gap permittivity and frequency. The axial propagation equation is

$$\tan^{-1}\left[\frac{\beta^h_{n,2}}{\beta^h_{n,1}}\tan(\beta^h_{n,1}h_1)\right] + \tan^{-1}\left[\frac{\beta^h_{n,2}}{\beta^h_{n,3}}\tan(\beta^h_{n,3}h_3)\right] + \beta^h_{n,2}h_2 - n\pi = 0,$$
$$n = 0, \pm1, \pm2, \pm3, ... \quad (118)$$

- Values of the propagation constant $\beta^h_{n,2}$ for each n define the radial wavenumber in the thin film $\zeta^h_n = \sqrt{\eta^h_n}$, where $\eta^h_n = k_0^2\epsilon'_{r,2} - (\beta^h_{n,2})^2$, which is an argument of the first governing equation,

$$\sum_{n=1}^{\infty}\left[\zeta^h_m J_0(\zeta^h_m a)K_1(\xi^h_n a) + \xi^h_n K_0(\xi^h_n a)J_1(\zeta^h_m a)\right] < Z^h_m, \sin(n\pi z/h) > B_n = 0. \quad (119)$$

- The first governing equation has the matrix form

$$\mathrm{M}(\epsilon'_{\mathbf{r,2}})\mathrm{B} = 0, \quad (120)$$

and the solution for $\epsilon'_{r,2}$, given frequency, (or frequency, given $\epsilon'_{r,2}$), is found from the determinant

$$det\left[\mathrm{M}(\epsilon'_{\mathbf{r,2}})\right] = 0. \quad (121)$$

- This last procedure allows the determination of the thin film permittivity $\epsilon'_{r,2}$, given the identified $TE_{0\gamma\nu}$ resonant frequency. Conversely, the $TE_{0\gamma\nu}$ resonant frequencies can be evaluated, given the thin film permittivity. Substitution of the permittivity $\epsilon'_{r,2}$ into the first governing equation allows the amplitude vector $\mathbf{B}$ to be found.

- Substitution of $\mathbf{B}$ into the following second governing equation,

$$\sum_{n=1}^{\infty} B_n K_1(\xi_n^h a) < Z_m^h, \sin(n\pi z/h) > \quad = \quad A_m J_1(\zeta_m^h a), \tag{122}$$

  permits the vector $\mathbf{A}$ to be found; that is, from the matrix equation

$$\mathbf{NB} = \mathbf{PA}, \tag{123}$$

$$\mathbf{A} = \mathbf{P}^{-1}\mathbf{NB} \tag{124}$$

- With $\mathbf{A}$ and $\mathbf{B}$, both the film permittivity $\epsilon'_{r,2}$ and the electric and magnetic field components are known, as well as partial electric filling factors and conductor plate losses. The thin-film loss tangent $\tan\delta_{tf}$ is then evaluated from

$$\tan\delta_{tf} \quad = \quad p_{e,tf}^{-1}\left(\frac{1}{Q_0} - \frac{1}{Q_p}\right), \tag{125}$$

  where

$$\frac{1}{Q_p} = p_{e,substrate}\tan\delta_{substrate} + \frac{1}{Q_c}, \tag{126}$$

  and Q_c^{-1} are the parallel plate conductor losses.

- Relative uncertainties in thin film permittivity and dielectric loss tangent can be determined numerically by evaluating the sensitivity (derivatives) of permittivity and dielectric loss tangent to given parameters and relative uncertainties of those parameters.

Once permittivity and dielectric loss characteristics of unpatterned thin films are evaluated, they can be used to examine the effects of substrates on thin-film dielectric behavior. They may also be used in advanced theoretical codes [14-16] to evaluate the propagation constants $\gamma = \alpha + j\beta$ for complex multi-layered thin film coplanar waveguide devices. These evaluated propagation constants can then be compared to microwave scattering parameter measurements for those devices.

RELATION OF THIN FILM DIELECTRIC PROPERTIES WITH PHYSICAL RELAXATION MECHANISMS

Accurately measured thin-film dielectric properties with a procedure such as that outlined above provides the basis for studying the physical relaxation mechanisms responsible for thin film electrical behavior. To see this, a thin film in an rf device may be generally characterized by its intrinsic complex admittance Y^*_{film}, which can be written as,

$$Y^*_{film} = G + j\omega C, \tag{127}$$

where G and C are the intrinsic conductance and capacitance of the thin-film structure determined by the real and imaginary part of Y^*_{film}. The dielectric loss tangent is given by

$$\tan\delta = \frac{G}{\omega C}, \tag{128}$$

and the $Q \times f$ product conventionally ascribed to bulk materials is

$$Q \times f = \frac{f}{\tan\delta} = \frac{2\pi f^2 C}{G}. \tag{129}$$

An interesting approach for evaluating the frequency domain response from the time domain response of a step-excited thin film, once parasitics of the test structure or test configuration have been removed, is to measure the time domain relaxation current J_r. The complex film admittance can be considered a complex capacitance, $Y^*_{film}(\omega) = j\omega(C'(\omega) - jC''(\omega))$, relatable to the frequency-dispersive and temperature-variable permittivity and dielectric loss tangent by the area and thickness of the film. The real and imaginary parts of the complex capacitance in the frequency domain are then given by the cosine and sine transforms of the relaxation current,

$$C'(\omega) = C'(\omega_1) + \frac{A}{V}\int_0^\infty J_r(t)[\cos(\omega t) - \cos(\omega_1 t)]dt, \tag{130}$$

$$C''(\omega) = \frac{A}{V}\int_0^\infty J_r \sin(\omega t)dt, \tag{131}$$

where V is the applied voltage, A is the area of the test film, and $C'(\omega_1)$ is the value of the capacitance at an arbitrary frequency from frequency domain measurements. The dielectric loss tangent is given by

$$\tan\delta = \frac{C''}{C'}, \tag{132}$$

where $C'' = G/\omega$. Equations (139) and (140) may be integrated over a finite time interval, with the early and late time responses yielding high-frequency and low-frequency dielectric characterization of the thin film structure. If use is made of the Curie-Schweidler law,

$$J_r(t) = J_0 t^{-x}, \tag{133}$$

where x <1, and the power law dependence is valid over the integration range, the real and imaginary parts of the complex capacitance in the frequency domain may be written in analytic form as

$$C'(\omega) = C'(\omega_1) + (\omega^{x-1} - \omega_1^{x-1}) \frac{J_0 A \Gamma(1-x) \sin(\pi x/2)}{V}, \tag{134}$$

$$C''(\omega) = \frac{J_0 A \Gamma(1-x) \cos(\pi x/2) \omega^{x-1}}{V}, \tag{135}$$

where $\Gamma(1-x)$ is the gamma function of $1-x$. The loss tangent in terms of the power law dependence of the relaxation current is

$$\tan\delta = \frac{J_0 A \Gamma(1-x) \cos(\pi x/2) \omega^{x-1}}{C'(\omega_1) V + J_0 A \Gamma(1-x) \sin(\pi x/2)(\omega^{x-1} - \omega_1^{x-1})}. \tag{136}$$

The applicability and physical mechanisms resulting in Curie-Schweidler behavior has been examined by Jonscher [17-19] and Fukuda, Numata, Aoki and Nishimura [20]. Jonscher has observed this power law dependence in many structurally disordered solids that are either glassy or crystalline. A natural variation in grain size in polycrystalline dielectric thin films could produce sufficient scatter in energy barrier across the film as a result of complete carrier depletion. Fukuda, Numata, Aoki and Nishimura have proposed that electrons from oxygen vacancies in interfacial thin film-substrate depletion regions are the origin of this power law dependence. In general, the nature of relaxation mechanisms for a wide spectrum of thin films need further study in order to engineer the dielectric properties at high frequency.

SUMMARY

A new procedure for in-plane microwave dielectric characterization of unpatterned thin films has been derived. In this method, the thin film and its substrate are used as an axially layered $TE_{0\gamma\nu}$ dielectric resonator. Specimens need not be metallized. This procedure permits dielectric characterization in the plane of the thin film over a tunable frequency range. With the introduction of a tunable gap between the thin film and upper ground plane of a parallel plate waveguide, the partial electric field energy filling factor in the specimen can be maximized, which enhances the sensitivity of the technique to thin film electrical properties.

Future work will involve numerical analysis of the theoretical derivations and experimental measurements focussed principally on high-permittivity ferroelectric thin films. The thin film dielectric properties will be correlated with structural, compositional, and surface morpological properties for microwave applications.

REFERENCES

[1] B.W. Hakki and P.D. Coleman,"A dielectric resonator method of measuring inductive capacities in the millimeter range," *IEEE Trans. Microwave Theory Tech.*, vol. MTT-8, pp. 402-410, 1960.

[2] W.E. Courtney, "Analysis and evaluation of a method of measuring the complex permittivity and permeability of microwave insulators," *IEEE Trans. Microwave theory Tech.*, vol. MTT-18, pp. 476-485, 1970.

[3] D. Kajfez and P. Guillon, *Dielectric Resonators.* Norwood, Massachusetts: Artech House, Inc., 1986.

[4] R. Courant and D. Hilbert, *Methods of Mathematical Physics.* New York: Interscience, 1965.

[5] B. Friedman, *Principles and Techniques of Applied Mathematics.* New York: John Wiley & Sons, 1956.

[6] H.B. Dwight, *Tables of Integrals and Other Mathematical Data.* New York: The Macmillan Company, 1972.

[7] L.B. Felson and N. Marcuvitz, *Radiation and Scattering of Waves.* Englewood Cliffs, N.J.: Prentice Hall, 1973.

[8] M. Abramowitz and I.A. Stegun, *Handbook of Mathematical Functions with Formulas, Graphs, and Mathematical Tables.* Washington, D.C.: National Bureau of Standards Applied Mathematics Series 55, 1964.

[9] Y. Kobayashi, N. Fukuoda, and S. Yoshida, "Resonant modes for a shielded dielectric resonator," *Electronics and Communications in Japan*, vol. 64-B, n. 11, pp. 46-51, 1981.

[10] J. Krupka, R.G. Geyer, and D. Cros, "Measurements of permittivity and the dielectric loss tangent of low loss dielectric materials with a dielectric resonator," *Proc., Mikon X International Microwave Conf.*, vol. 2, pp. 567-572, 1994.

[11] H. A. Wheeler, "Formulas for the skin effect," *Proc., IRE*, vol. 30, pp. 412-424, 1942. [12] D. Kajfez, "Incremental frequency rule for computing the Q-factor of a shielded TE_{0mp} dielectric resonator," *IEEE Trans. Microwave Theory Tech.*, vol.

MTT-32, pp. 941-943, 1984.

[13] I.S. Gradshteyn and I.M. Ryshik, *Table of Integrals, Series, and Products.* New York: Academic Press, 1980.

[14] C.M. Krowne, "Use of self-adjoint operators for implicit 3D dyadic Green's function for inhomogeneous planar ferrite circulator with vertically layered external material employing mode-matching," *IEEE Trans. Microwave Theory Tech.*, vol. MTT-46, pp. 359-377, 1998.

[15] C.M. Krowne, "Theoretical considerations for full-wave electromagnetic medium interactions in layered structures with ferroelectric or ferromagnetic materials," *Proc. SPIE*, vol. 4097, pp. 70-84, 2000.

[16] C.M. Krowne, S.W. Kirchoefer, and J.M. Pond, "Anisotropic permittivity extraction from phase propagation measurements using an anisotropic full-wave Green's function solver for coplanar ferroelectric thin film devices," *IEEE Microwave Theory Tech. Dig.*, pp. 1193-1196, 2000.

[17] A.K. Jonscher, "Universal dielectric response," *Nature*, vol. 267, p. 673, 1977.

[18] A.K. Jonscher, "The universal dielectric dispersion in low mobility solids," *J. Mater. Sci. Lett.*, vol. 4, pp. 980-981, 1985.

[19] A.K. Jonscher, "The universal dielectric response and its physical significance," *IEEE Trans. Electrical Ins.*, vol. 27, pp. 407-423, 1992.

[20] Y. Fukuda, K. Numata, K. Aoki, and Nishimura, "Origin of dielectric relaxation observed for $Ba_{.5}Sr_{.5}TiO_3$ thin-film capacitor," *Japanese J. Appl. Phys., Part 1-Regular Papers, Short Notes and Review Papers*, vol. 35, pp. 5178-5180, 1996.

Appendix A: Unnormalized Axial Eigenfunctions

General solutions for the unnormalized axial eigenfunctions may be written as

$$Z^h_{n,1}(z) = a_n \sin(\beta^h_{n,1} z), \qquad 0 \le z \le h_1, \tag{A-1}$$

$$Z^h_{n,2}(z) = b_n \sin(\beta^h_{n,2} z) + c_n \cos(\beta^h_{n,2} z), \qquad h_1 \le z \le h_1 + h_2, \tag{A-2}$$

and

$$Z^h_{n,3}(z) = d_n \sin\left[\beta^h_{n,3}(z-h)\right], \qquad h_1 + h_2 \le z \le h, \tag{A-3}$$

where $\beta^h_{n,1} = (k_0^2 \epsilon'_{r,1} - \eta_n^h)^{1/2}$ or $\beta^h_{n,1} = j(\eta_n^h - k_0^2 \epsilon'_{r,1})^{1/2}$; $\beta^h_{n,2} = (k_0^2 \epsilon'_{r,2} - \eta_n^h)^{1/2}$ or $\beta^h_{n,2} = j(\eta_n^h - k_0^2 \epsilon'_{r,2})^{1/2}$; $\beta^h_{n,3} = (k_0^2 - \eta_n^h)^{1/2}$ or $\beta^h_{n,3} = j(\eta_n^h - k_0^2)^{1/2}$; and $h = h_1 + h_2 + h_3$. Continuity of the azimuthal electric field and radial magnetic field at $z = h_1$ yields

$$\begin{aligned} a_n \sin(\beta^h_{n,1} h_1) &= b_n \sin(\beta^h_{n,2} h_1) + c_n \cos(\beta^h_{n,2} h_1), \\ a_n \beta^h_{n,1} \cos(\beta^h_{n,1} h_1) &= b_n \beta^h_{n,2} \cos(\beta^h_{n,2} h_1) - c_n \beta^h_{n,2} \sin(\beta^h_{n,2} h_1). \end{aligned}$$

Solving for b_n and c_n, we obtain,

$$b_n = \frac{a_n}{\beta^h_{n,2}} \left[\beta^h_{n,2} \sin(\beta^h_{n,1} h_1) \sin(\beta^h_{n,2} h_1) + \beta^h_{n,1} \cos(\beta^h_{n,1} h_1) \cos(\beta^h_{n,2} h_1)\right], \tag{A-4}$$

and

$$c_n = \frac{a_n}{\beta^h_{n,2}} \left[\beta^h_{n,2} \sin(\beta^h_{n,1} h_1) \cos(\beta^h_{n,2} h_1) - \beta^h_{n,1} \sin(\beta^h_{n,2} h_1) \cos(\beta^h_{n,1} h_1)\right]. \tag{A-5}$$

Hence

$$\begin{aligned} Z^h_{n,2}(z) &= b_n \sin(\beta^h_{n,2} z) + c_n \cos(\beta^h_{n,2} z) \\ &= a_n \Bigg(\left[\frac{\beta^h_{n,2} \sin(\beta^h_{n,1} h_1) \sin(\beta^h_{n,2} h_1) + \beta^h_{n,1} \cos(\beta^h_{n,1} h_1) \cos(\beta^h_{n,2} h_1)}{\beta^h_{n,2}} \right] \sin(\beta^h_{n,2} z) \\ &\quad + \left[\frac{\beta^h_{n,2} \sin(\beta^h_{n,1} h_1) \cos(\beta^h_{n,2} h_1) - \beta^h_{n,1} \sin(\beta^h_{n,2} h_1) \cos(\beta^h_{n,1} h_1)}{\beta^h_{n,2}} \right] \cos(\beta^h_{n,2} z) \Bigg) \\ &= \frac{a_n}{\beta^h_{n,2}} \Big(\beta^h_{n,2} \left[\sin(\beta^h_{n,1} h_1) \sin(\beta^h_{n,2} h_1) \sin(\beta^h_{n,2} z) + \sin(\beta^h_{n,1} h_1) \cos(\beta^h_{n,2} h_1) \cos(\beta^h_{n,2} z) \right] \\ &\quad + \beta^h_{n,1} \left[\cos(\beta^h_{n,1} h_1) \cos(\beta^h_{n,2} h_1) \sin(\beta^h_{n,2} z) - \sin(\beta^h_{n,2} h_1) \cos(\beta^h_{n,1} h_1) \cos(\beta^h_{n,2} z) \right] \Big) \end{aligned}$$

or

$$Z^h_{n,2}(z) = \frac{a_n}{\beta^h_{n,2}}(\beta^h_{n,2}\sin(\beta^h_{n,1}h_1)\left[\sin(\beta^h_{n,2}h_1)\sin(\beta^h_{n,2}z)+\cos(\beta^h_{n,2}h_1)\cos(\beta^h_{n,2}z)\right]$$
$$+\beta^h_{n,1}\cos(\beta^h_{n,1}h_1)\left[\cos(\beta^h_{n,2}h_1)\sin(\beta^h_{n,2}z)-\sin(\beta^h_{n,2}h_1)\cos(\beta^h_{n,2}z)\right]).$$

Using the trigonometric identities [6]

$$\cos(x-y) = \cos x\cos y+\sin x\sin y,$$
$$\sin(x-y) = \sin x\cos y-\cos x\sin y,$$

we can write

$$\left[\sin(\beta^h_{n,2}h_1)\sin(\beta^h_{n,2}z)+\cos(\beta^h_{n,2}h_1)\cos(\beta^h_{n,2}z)\right] = \cos\left[\beta^h_{n,2}(z-h_1)\right],$$

and

$$\left[\cos(\beta^h_{n,2}h_1)\sin(\beta^h_{n,2}z)-\sin(\beta^h_{n,2}h_1)\cos(\beta^h_{n,2}z)\right] = \sin\left[\beta^h_{n,2}(z-h_1)\right],$$

so that

$$Z^h_{n,2}(z) = \frac{a_n}{\beta^h_{n,2}}\left[\beta^h_{n,2}\sin(\beta^h_{n,1}h_1)\cos\left[\beta^h_{n,2}(z-h_1)\right]+\beta^h_{n,1}\cos(\beta^h_{n,1}h_1)\sin\left[\beta^h_{n,2}(z-h_1)\right]\right]$$
$$= a_n\frac{\beta^h_{n,1}}{\beta^h_{n,2}}\cos(\beta^h_{n,1}h_1)\left[\frac{\beta^h_{n,2}}{\beta^h_{n,1}}\frac{\sin(\beta^h_{n,1}h_1)}{\cos(\beta^h_{n,1}h_1)}\cos\left[\beta^h_{n,2}(z-h_1)\right]+\sin\left[\beta^h_{n,2}(z-h_1)\right]\right],$$

or

$$Z^h_{n,2}(z) = a_n\frac{\beta^h_{n,1}}{\beta^h_{n,2}}\cos(\beta^h_{n,1}h_1)\left(\tan\Phi^h_n\cos\left[\beta^h_{n,2}(z-h_1)\right]+\sin\left[\beta^h_{n,2}(z-h_1)\right]\right), \quad (A-6)$$

where

$$\tan\Phi^h_n = \frac{\beta^h_{n,2}}{\beta^h_{n,1}}\frac{\sin(\beta^h_{n,1}h_1)}{\cos(\beta^h_{n,1}h_1)} = \frac{\beta^h_{n,2}}{\beta^h_{n,1}}\tan(\beta^h_{n,1}h_1). \quad (A-7)$$

We may determine d_n in terms of a_n by invoking continuity of the azimuthal electric field or radial magnetic field at $z = h_1 + h_2$; that is,

$$Z^h_{n,2}(z) = Z^h_{n,3}(z), \qquad z = h_1+h_2$$
$$\frac{dZ^h_{n,2}(z)}{dz} = \frac{dZ^h_{n,3}(z)}{dz}, \qquad z = h_1+h_2.$$

From continuity of the azimuthal electric field,

$$a_n \frac{\beta_{n,1}^h}{\beta_{n,2}^h} \cos(\beta_{n,1}^h h_1) \left[\tan \Phi_n^h \cos(\beta_{n,2}^h h_2) + \sin(\beta_{n,2}^h h_2)\right] = -d_n \sin(\beta_{n,3}^h h_3)$$

so that

$$\begin{aligned} d_n &= -a_n \frac{\beta_{n,1}^h}{\beta_{n,2}^h} \frac{\cos(\beta_{n,1}^h h_1)}{\sin(\beta_{n,3}^h h_3)} \left[\tan \Phi_n^h \cos(\beta_{n,2}^h h_2) + \sin(\beta_{n,2}^h h_2)\right] \\ &= -a_n \sin(\beta_{n,2}^h h_2) \frac{\beta_{n,1}^h}{\beta_{n,2}^h} \frac{\cos(\beta_{n,1}^h h_1)}{\sin(\beta_{n,3}^h h_3)} \left[\tan \Phi_n^h \cot(\beta_{n,2}^h h_2) + 1\right]. \qquad (A-8) \end{aligned}$$

In a similar manner, we could use continuity of the radial magnetic field at $z = h_1 + h_2$ to give

$$a_n \beta_{n,1}^h \cos(\beta_{n,1}^h h_1) \left[\cos(\beta_{n,2}^h h_2) - \tan \Phi_n^h \sin(\beta_{n,2}^h h_2)\right] = d_n \beta_{n,3}^h \cos(\beta_{n,3}^h h_3).$$

or

$$d_n = a_n \cos(\beta_{n,2}^h h_2) \frac{\beta_{n,1}^h}{\beta_{n,3}^h} \frac{\cos(\beta_{n,1}^h h_1)}{\cos(\beta_{n,3}^h h_3)} \left[1 - \tan \Phi_n^h \tan(\beta_{n,2}^h h_2)\right]. \qquad (A-9)$$

If we use the last boundary condition, we can write the unnormalized eigenfunction $Z_{n,3}(z)$ in the gap as

$$\begin{aligned} Z_{n,3}^h(z) &= d_n \sin\left[\beta_{n,3}^h (z-h)\right] = -d_n \sin\left[\beta_{n,3}^h (h-z)\right] \\ &= a_n \cos(\beta_{n,2}^h h_2) \frac{\beta_{n,1}^h}{\beta_{n,3}^h} \frac{\cos(\beta_{n,1}^h)}{\cos(\beta_{n,3}^h)} \left[\tan \Phi_n^h \tan(\beta_{n,2}^h h_2) - 1\right] \\ &\quad \cdot \sin\left[\beta_{n,3}^h (h-z)\right]. \qquad (A-10) \end{aligned}$$

Appendix B: Real Φ_n and Ψ_n for Evanescent Fields in Substrate and Tuning Gap

It may readily be shown that Φ_n and Ψ_n in the axial wave propagation constant eq (76) are always real for real $\beta^h_{n,2}$, even if $\beta^h_{n,1}$ and $\beta^h_{n,3}$ are imaginary.

Case 1: $\beta^h_{n,1}$ Pure Imaginary

To see this, note that if $\beta^h_{n,1} = j(\eta^h_n - k_0^2\epsilon'_{r,1})^{1/2}$ where $\eta^h_n - k_0^2\epsilon'_{r,1}$ is real, then $\beta^h_{n,1} = j \mid \beta^h_{n,1} \mid$ is pure imaginary. Hence

$$\begin{aligned}\tan\Phi_n &= \frac{\beta^h_{n,2}}{j \mid \beta^h_{n,1} \mid}\tan(j \mid \beta^h_{n,1} \mid h_1) = \frac{\beta^h_{n,2}}{j \mid \beta^h_{n,1} \mid} j\tanh(\mid \beta^h_{n,1} \mid h_1) \\ &= \frac{\beta^h_{n,2}}{\mid \beta^h_{n,1} \mid}\tanh(\mid \beta^h_{n,1} \mid h_1), \qquad (B-1)\end{aligned}$$

which is real if $\beta^h_{n,2}$ is real. In this case the axial wave propagation constant equation becomes,

$$\tan^{-1}\left[\frac{\beta^h_{n,2}}{\mid \beta^h_{n,1} \mid}\tanh(\mid \beta^h_{n,1} \mid h_1)\right] + \tan^{-1}\left[\frac{\beta^h_{n,2}}{\beta^h_{n,3}}\tan(\beta^h_{n,3}h_3)\right] + \beta^h_{n,2}h_2 - n\pi = 0,$$
$$n = 0, \pm 1, \pm 2, \pm 3, ... \qquad (B-2)$$

Case 2: $\beta^h_{n,3}$ Pure Imaginary

If $\beta^h_{n,3} = j(\eta^h_n - k_0^2)^{1/2}$, where $\eta^h_n - k_0^2$ is real, then $\beta^h_{n,3} = j \mid \beta^h_{n,3} \mid$ is pure imaginary. In this case,

$$\begin{aligned}\tan\Psi_n &= \frac{\beta^h_{n,2}}{j \mid \beta^h_{n,3} \mid}\tan(j \mid \beta^h_{n,3} \mid h_3) = \frac{\beta^h_{n,2}}{j \mid \beta^h_{n,3} \mid} j\tanh(\mid \beta^h_{n,3} \mid h_3) \\ &= \frac{\beta^h_{n,2}}{\mid \beta^h_{n,3} \mid}\tanh(\mid \beta^h_{n,3} \mid h_3), \qquad (B-3)\end{aligned}$$

which is real provided $\beta^h_{n,2}$ is real. The axial wave propagation constant equation becomes

$$\tan^{-1}\left[\frac{\beta^h_{n,2}}{\beta^h_{n,1}}\tan(\beta^h_{n,1}h_1)\right] + \tan^{-1}\left[\frac{\beta^h_{n,2}}{\mid \beta^h_{n,3} \mid}\tanh(\mid \beta^h_{n,3} \mid h_3)\right] + \beta^h_{n,2}h_2 - n\pi = 0,$$
$$n = 0, \pm 1, \pm 2, \pm 3, ... \qquad (B-4)$$

Case 3: $\beta^h_{n,1}$, $\beta^h_{n,3}$ Pure Imaginary

For this case the axial propagation constant eq (76) becomes,

$$\tan^{-1}\left[\frac{\beta^h_{n,2}}{\mid \beta^h_{n,1} \mid}\tanh(\mid \beta^h_{n,1} \mid h_1)\right] + \tan^{-1}\left[\frac{\beta^h_{n,2}}{\mid \beta^h_{n,3} \mid}\tanh(\mid \beta^h_{n,3} \mid h_3)\right] + \beta^h_{n,2}h_2 - n\pi = 0,$$
$$n = 0, \pm 1, \pm 2, \pm 3, ... \qquad (B-5)$$

which remains real for real $\beta^h_{n,2}$.

Appendix C: Evaluation of Integrals I_1, I_2, and I_3 for Normalization Constant C_n

The integrals I_1, I_2, and I_3 are in standard form and may be evaluated with the use of the following definite integrals [6],

$$\int \cos^2 x dx = \frac{x}{2} + \frac{\sin x \cos x}{2}, \qquad (C-1)$$

$$\int \sin x \cos x dx = \frac{\sin^2 x}{2}, \qquad (C-2)$$

and

$$\int \sin^2 x dx = \frac{x}{2} - \frac{\sin x \cos x}{2}. \qquad (C-3)$$

Hence

$$\begin{aligned} I_1 &= \int_0^{h_1} \sin^2(\beta_{n,1}^h z) dz = \frac{1}{\beta_{n,1}^h} \int_0^{\beta_{n,1}^h h_1} \sin^2 v dv \\ &= \frac{1}{\beta_{n,1}^h} \left[\frac{v}{2} - \frac{\sin v \cos v}{2} \right]_0^{\beta_{n,1}^h h_1}, \end{aligned}$$

or

$$I_1 = \frac{1}{\beta_{n,1}^h} \left[\frac{\beta_{n,1}^h h_1}{2} - \frac{\sin(\beta_{n,1}^h h_1)\cos(\beta_{n,1}^h h_1)}{2} \right]. \qquad (C-4)$$

$$\begin{aligned} I_2 &= \int_{h_1}^{h_1+h_2} \left(\tan\Phi_n \cos\left[\beta_{n,2}^h (z-h_1)\right] + \sin\left[\beta_{n,2}^h (z-h_1)\right] \right)^2 dz \\ &= \int_0^{h_2} \left(\tan\Phi_n \cos\left[\beta_{n,2}^h v\right] + \sin\left[\beta_{n,2}^h v\right] \right)^2 dv \\ &= \int_0^{h_2} [\tan^2\Phi_n \cos^2(\beta_{n,2}^h v) + 2\tan\Phi_n \cos(\beta_{n,2}^h v)\sin(\beta_{n,2}^h v) + \sin^2(\beta_{n,2}^h v)] dv \\ &= \tan^2\Phi_n \int_0^{h_2} \cos^2(\beta_{n,2}^h v) dv + 2\tan\Phi_n \int_0^{h_2} \cos(\beta_{n,2}^h v)\sin(\beta_{n,2}^h v) dv \\ &\qquad + \int_0^{h_2} \sin^2(\beta_{n,2}^h v) dv \\ &= \tan^2\Phi_n \left(\frac{1}{\beta_{n,2}^h} \left[\frac{v}{2} + \frac{\sin v \cos v}{2} \right]_0^{\beta_{n,2}^h h_2} \right) \end{aligned}$$

$$
\begin{aligned}
&+2\tan\Phi_n\left(\frac{1}{\beta^h_{n,2}}\left[\frac{\sin^2 v}{2}\right]_0^{\beta^h_{n,2}h_2}\right)\\
&+\frac{1}{\beta^h_{n,2}}\left[\frac{v}{2}-\frac{\sin v\cos v}{2}\right]_0^{\beta^h_{n,2}h_2}\\
= \;& \frac{\tan^2\Phi_n}{2\beta^h_{n,2}}\left[\beta^h_{n,2}h_2+\sin(\beta^h_{n,2}h_2)\cos(\beta^h_{n,2}h_2)\right]\\
&+\frac{\tan\Phi_n}{\beta^h_{n,2}}\sin^2(\beta^h_{n,2}h_2)\\
&+\frac{1}{2\beta^h_{n,2}}\left[\beta^h_{n,2}h_2-\sin(\beta^h_{n,2}h_2)\cos(\beta^h_{n,2}h_2)\right]
\end{aligned}
$$

or

$$
\begin{aligned}
I_2 \;=\; & \frac{h_2}{2}\left(\tan^2\Phi_n+1\right)+\frac{\sin(\beta^h_{n,2}h_2)\cos(\beta_{n,2}h_2)}{2\beta^h_{n,2}}\left(\tan^2\Phi_n-1\right)\\
&+\tan\Phi_n\frac{\sin^2(\beta^h_{n,2}h_2)}{\beta^h_{n,2}}. \qquad (C-5)
\end{aligned}
$$

The third integral is

$$
\begin{aligned}
I_3 \;=\; & \int_{h_1+h_2}^{h}\sin^2\left[\beta^h_{n,3}(h-z)\right]dz\\
=\; & -\frac{1}{\beta^h_{n,3}}\int_{\beta^h_{n,3}h_3}^{0}\sin^2 v\,dv=\frac{1}{\beta^h_{n,3}}\int_0^{\beta^h_{n,3}h_3}\sin^2 v\,dv\\
=\; & \frac{1}{2}\left[h_3-\frac{\sin(\beta^h_{n,3}h_3)\cos(\beta_{n,3}h_3)}{\beta^h_{n,3}}\right]. \qquad (C-6)
\end{aligned}
$$

Appendix D: Evaluation of Integrals $\tilde{I}_1$, $\tilde{I}_2$, and $\tilde{I}_3$ for Mode-Matched Solution Inner Products

The integrals $\tilde{I}_1$, $\tilde{I}_2$, and $\tilde{I}_3$ in eqs (93), (94), and (95) are needed for evaluation of the inner products $< Z_m^h, \sin(n\pi z/h) >$. For these evaluations, the following indefinite integrals are used [13]:

$$\int \sin(ax+b)\sin(cx+d)dx = \frac{\sin\left[(a-c)x+b-d\right]}{2(a-c)} - \frac{\sin\left[(a+c)x+b+d\right]}{2(a+c)}, \quad a^2 \neq c^2, \qquad (D-1)$$

and

$$\int \sin(ax+b)\cos(cx+d)dx = -\frac{\cos\left[(a-c)x+b-d\right]}{2(a-c)} - \frac{\cos\left[(a+c)x+b+d\right]}{2(a+c)}, \quad a^2 \neq c^2. \qquad (D-2)$$

The first integral $\tilde{I}_1$ is given by

$$\begin{aligned}
\tilde{I}_1 &= \int_0^{h_1} \sin(\beta_{m,1}^h z)\sin(n\pi z/h)dz \\
&= \frac{\sin\left[(\beta_{m,1}^h - n\pi/h)h_1\right]}{2(\beta_{m,1}^h - n\pi/h)} - \frac{\sin\left[(\beta_{m,1}^h + n\pi/h)h_1\right]}{2(\beta_{m,1}^h + n\pi/h)} \\
&= \frac{\sin(\beta_{m,1}^h h_1)\cos(\frac{n\pi h_1}{h}) - \cos(\beta_{m,1}^h h_1)\sin(\frac{n\pi h_1}{h})}{2(\beta_{m,1}^h - n\pi/h)} \\
&\quad - \frac{\sin(\beta_{m,1}^h h_1)\cos(\frac{n\pi h_1}{h}) + \cos(\beta_{m,1}^h h_1)\sin(\frac{n\pi h_1}{h})}{2(\beta_{m,1}^h + n\pi/h)} \qquad (D-3)
\end{aligned}$$

or

$$\tilde{I}_1 = h\left(\frac{\beta_{m,1}^h h\cos(\beta_{m,1}^h h_1)\sin(\frac{n\pi h_1}{h}) - n\pi\sin(\beta_{m,1}^h h_1)\cos(\frac{n\pi h_1}{h})}{(n\pi)^2 - (\beta_{m,1}^h h)^2}\right). \qquad (D-4)$$

$\tilde{I}_2$ is given by

$$\begin{aligned}
\tilde{I}_2 &= \tan\Phi_m \int_{h_1}^{h_1+h_2} \cos\left[\beta_{m,2}^h(z-h_1)\right]\sin(\frac{n\pi z}{h})dz \\
&\quad + \int_{h_1}^{h_1+h_2} \sin\left[\beta_{m,2}^h(z-h_1)\right]\sin(\frac{n\pi z}{h})dz \\
&= \tan\Phi_m \tilde{I}_{2a} + \tilde{I}_{2b}, \qquad (D-5)
\end{aligned}$$

where

$$\begin{aligned}
\tilde{I}_{2a} &= \int_{h_1}^{h_1+h_2} \sin(\frac{n\pi z}{h}) \cos\left[\beta_{m,2}^h z - \beta_{m,2}^h h_1\right] dz \\
&= \frac{\cos(\frac{n\pi h_1}{h}) - \cos\left[\frac{n\pi}{h}(h_1+h_2) - \beta_{m,2}^h h_2\right]}{2(\frac{n\pi}{h} - \beta_{m,2}^h)} \\
&\quad + \frac{\cos(\frac{n\pi h_1}{h} - \cos\left[\frac{n\pi}{h}(h_1+h_2) + \beta_{m,2}^h h_2\right]}{2(\frac{n\pi}{h} + \beta_{m,2}^h)} \\
&= \frac{h}{2}\Big(\frac{\cos(\frac{n\pi h_1}{h}) - \cos\left[\frac{n\pi(h_1+h_2)}{h}\right]\cos(\beta_{m,2}^h h_2) - \sin\left[\frac{n\pi(h_1+h_2)}{h}\right]\sin(\beta_{m,2}^h h_2)}{n\pi - \beta_{m,2}^h h} \\
&\quad + \frac{\cos(\frac{n\pi h_1}{h}) - \cos\left[\frac{n\pi(h_1+h_2)}{h}\right]\cos(\beta_{m,2}^h h_2) + \sin\left[\frac{n\pi(h_1+h_2)}{h}\right]\sin(\beta_{m,2}^h h_2)}{n\pi + \beta_{m,2}^h h}\Big),
\end{aligned} \tag{D-6}$$

or

$$\begin{aligned}
\tilde{I}_{2a} &= h\Big(\frac{n\pi\left[\cos(\frac{n\pi h_1}{h}) - \cos\left(\frac{n\pi(h_1+h_2)}{h}\right)\cos(\beta_{m,2}^h h_2)\right]}{(n\pi)^2 - (\beta_{m,2}^h h)^2} \\
&\quad - \frac{\beta_{m,2}^h h \sin\left[\frac{n\pi(h_1+h_2)}{h}\right]\sin(\beta_{m,2}^h h_2)}{(n\pi)^2 - (\beta_{m,2}^h h)^2}\Big).
\end{aligned} \tag{D-7}$$

Similarly,

$$\begin{aligned}
\tilde{I}_{2b} &= \int_{h_1}^{h_1+h_2} \sin\left[\beta_{m,2}^h z - \beta_{m,2}^h h_1\right] \sin(\frac{n\pi z}{h}) dz \\
&= \frac{\sin\left[\beta_{m,2}^h h_2 - \frac{n\pi}{h}(h_1+h_2)\right]}{2(\beta_{m,2}^h - n\pi/h)} + \frac{\sin(\frac{n\pi h_1}{h})}{2(\beta_{m,2}^h - n\pi/h)} \\
&\quad - \frac{\sin\left[\beta_{m,2}^h h_2 + \frac{n\pi}{h}(h_1+h_2)\right]}{2(\beta_{m,2}^h + \frac{n\pi}{h})} + \frac{\sin(\frac{n\pi h_1}{h})}{2(\beta_{m,2}^h + n\pi/h)} \\
&= \frac{h}{2}\Big(\frac{\sin(\beta_{m,2}^h h_2)\cos\left[\frac{n\pi(h_1+h_2)}{h}\right] - \cos(\beta_{m,2}^h h_2)\sin\left[\frac{n\pi(h_1+h_2)}{h}\right]}{\beta_{m,2}^h - n\pi} \\
&\quad + \frac{\sin(\frac{n\pi h_1}{h})}{\beta_{m,2}^h h - n\pi} + \frac{\sin(\frac{n\pi h_1}{h})}{\beta_{m,2}^h h + n\pi}
\end{aligned}$$

$$-\frac{\sin(\beta^h_{m,2}h_2)\cos\left[\frac{n\pi(h_1+h_2)}{h}\right]+\cos(\beta^h_{m,2}h_2)\sin\left[\frac{n\pi(h_1+h_2)}{h}\right]}{\beta^h_{m,2}h+n\pi}), \qquad (D-8)$$

or

$$\begin{aligned}\tilde{I}_{2b} &= h[\frac{\beta^h_{m,2}h\left(\cos(\beta^h_{m,2}h_2)\sin\left[\frac{n\pi(h_1+h_2)}{h}\right]-\sin(\frac{n\pi h_1}{h})\right)}{(n\pi)^2-(\beta^h_{m,2}h)^2} \\ &\quad -\frac{n\pi\sin(\beta^h_{m,2}h_2)\cos\left[\frac{n\pi(h_1+h_2)}{h}\right]}{(n\pi)^2-(\beta^h_{m,2}h)^2}]. \qquad (D-9)\end{aligned}$$

Lastly,

$$\begin{aligned}\tilde{I}_3 &= \int_{h_1+h_2}^{h}\sin\left(\beta^h_{m,3}h-\beta^h_{m,3}z\right)\sin(\frac{n\pi z}{h})dz \\ &= \frac{h}{2}[\frac{\sin\left[\beta^h_{m,3}h-(\frac{n\pi}{h}+\beta^h_{m,3})h\right]}{-(\beta^h_{m,3}h+n\pi)}+\frac{\sin\left[\beta^h_{m,3}h-(\frac{n\pi}{h}+\beta^h_{m,3})(h_1+h_2)\right]}{\beta^h_{m,3}h+n\pi} \\ &\quad -\frac{\sin\left[\beta^h_{m,3}h+(\frac{n\pi}{h}-\beta^h_{m,3})h\right]}{n\pi-\beta^h_{m,3}h}+\frac{\sin\left[\beta^h_{m,3}h+(\frac{n\pi}{h}-\beta^h_{m,3})(h_1+h_2)\right]}{n\pi-\beta^h_{m,3}h}] \\ &= \frac{h}{2}[\frac{\sin(\beta^h_{m,3}h_3)\cos\left[\frac{n\pi}{h}(h_1+h_2)\right]-\cos(\beta^h_{m,3}h_3)\sin\left[\frac{n\pi}{h}(h_1+h_2)\right]}{n\pi+\beta^h_{m,3}h} \\ &\quad +\frac{\sin(\beta^h_{m,3}h_3)\cos\left[\frac{n\pi}{h}(h_1+h_2)\right]+\cos(\beta^h_{m,3}h_3)\sin\left[\frac{n\pi}{h}(h_1+h_2)\right]}{n\pi-\beta^h_{m,3}h}], \quad (D-10)\end{aligned}$$

or

$$\begin{aligned}\tilde{I}_3 &= h[\frac{n\pi\sin(\beta^h_{m,3}h_3)\cos\left[\frac{n\pi}{h}(h_1+h_2)\right]}{(n\pi)^2-(\beta^h_{m,3}h)^2} \\ &\quad +\frac{\beta^h_{m,3}h\cos(\beta^h_{m,3}h_3)\sin\left[\frac{n\pi}{h}(h_1+h_2)\right]}{(n\pi)^2-(\beta^h_{m,3}h)^2}]. \qquad (D-11)\end{aligned}$$

*U.S. GPO 2002-0-773-018/40216

NIST Technical Publications

Periodical

Journal of Research of the National Institute of Standards and Technology—Reports NIST research and development in metrology and related fields of physical science, engineering, applied mathematics, statistics, biotechnology, and information technology. Papers cover a broad range of subjects, with major emphasis on measurement methodology and the basic technology underlying standardization. Also included from time to time are survey articles on topics closely related to the Institute's technical and scientific programs. Issued six times a year.

Nonperiodicals

Monographs—Major contributions to the technical literature on various subjects related to the Institute's scientific and technical activities.

Handbooks—Recommended codes of engineering and industrial practice (including safety codes) developed in cooperation with interested industries, professional organizations, and regulatory bodies.

Special Publications—Include proceedings of conferences sponsored by NIST, NIST annual reports, and other special publications appropriate to this grouping such as wall charts, pocket cards, and bibliographies.

National Standard Reference Data Series—Provides quantitative data on the physical and chemical properties of materials, compiled from the world's literature and critically evaluated. Developed under a worldwide program coordinated by NIST under the authority of the National Standard Data Act (Public Law 90-396). NOTE: The Journal of Physical and Chemical Reference Data (JPCRD) is published bimonthly for NIST by the American Institute of Physics (AIP). Subscription orders and renewals are available from AIP, P.O. Box 503284, St. Louis, MO 63150-3284.

Building Science Series—Disseminates technical information developed at the Institute on building materials, components, systems, and whole structures. The series presents research results, test methods, and performance criteria related to the structural and environmental functions and the durability and safety characteristics of building elements and systems.

Technical Notes—Studies or reports which are complete in themselves but restrictive in their treatment of a subject. Analogous to monographs but not so comprehensive in scope or definitive in treatment of the subject area. Often serve as a vehicle for final reports of work performed at NIST under the sponsorship of other government agencies.

Voluntary Product Standards—Developed under procedures published by the Department of Commerce in Part 10, Title 15, of the Code of Federal Regulations. The standards establish nationally recognized requirements for products, and provide all concerned interests with a basis for common understanding of the characteristics of the products. NIST administers this program in support of the efforts of private-sector standardizing organizations.

Order the **following** *NIST publications—FIPS and NISTIRs—from the National Technical Information Service, Springfield, VA 22161.*

Federal Information Processing Standards Publications (FIPS PUB)—Publications in this series collectively constitute the Federal Information Processing Standards Register. The Register serves as the official source of information in the Federal Government regarding standards issued by NIST pursuant to the Federal Property and Administrative Services Act of 1949 as amended, Public Law 89-306 (79 Stat. 1127), and as implemented by Executive Order 11717 (38 FR 12315, dated May 11, 1973) and Part 6 of Title 15 CFR (Code of Federal Regulations).

NIST Interagency or Internal Reports (NISTIR)—The series includes interim or final reports on work performed by NIST for outside sponsors (both government and nongovernment). In general, initial distribution is handled by the sponsor; public distribution is handled by sales through the National Technical Information Service, Springfield, VA 22161, in hard copy, electronic media, or microfiche form. NISTIR's may also report results of NIST projects of transitory or limited interest, including those that will be published subsequently in more comprehensive form.

U.S. Department of Commerce
National Institute of Standards and Technology
325 Broadway
Boulder, Colorado 80305-3328

Official Business
Penalty for Private Use, $300